Engineering Science and Technology, an International Journal xxx (xxxx) xxx

HOSTED BY

ELSEVIER

Contents lists available at ScienceDirect

Engineering Science and Technology, an International Journal

journal homepage: www.elsevier.com/locate/jestch

Full Length Article

A novel two-stage distributed structure for reactive power control

Mohamadreza Hashemi *, Mohammad Haddad Zarif

Shahrood University of Technology, Shahrood, Iran

ARTICLE INFO

Article history:
Received 29 September 2018
Revised 1 March 2019
Accepted 7 March 2019
Available online xxxx

Keywords:
Optimal Reactive Power Dispatch (ORPD)
Distributed control structure
Partitioning approach
Distributed Energy Resources (DER)

ABSTRACT

In this paper, a new two-stage approach has been presented for the reactive power control of power systems. In the first stage, the transmission network is divided into several parts using a partitioning approach based on graph concept. In the second stage, a hierarchical distributed framework based on a System of Systems (SoS) concept has been proposed for optimal reactive power dispatch. In this structure, every section of the grid is controlled by a smart agent. Agents are interconnected and exchange the required data via a telecommunication network. In this paper, the amounts of active and reactive power exchanged between agents are considered as boundary and common parameters. Our proposed method is implemented on the IEEE 118-bus network connected to 7 active power distribution networks. The results are compared to the ones obtained from a distributed method based on an Incident Command System (ICS) and a centralized control method. It turns out that the proposed method outperforms the other two competing methods.

1. Introduction

The ever-increasing advances in power electronics and utilization of electricity in industry necessitated alterations in power distribution systems in various countries, due to altering the operational strategies. Consequently, energy management is addressed at the highest levels of technology and engineering. It is studied as a major economic investment and commodity. Thus, one of the main objectives for power systems operators is the economic and safe operation. To this end, optimal scheduling and performance of the power systems are required. They have recently attracted the attention of many researchers.

One of the tools to achieve the optimal performance and utilization of power systems is the Optimal Reactive Power Dispatch (ORPD). The problem of ORPD is a part of power system optimization problems in which, based on a series of constraints and control variables, specific objective functions are optimized. A review of the literature reveals three objective functions, as follows [1–4]: (i) improving the voltage profile; (ii) increasing the voltage stability margin; (iii) reducing active power losses. Thus, it is evident that reactive power significantly affects the major parameters of power systems operation.

There are different methods to solve ORPD optimization problems. Typical classification of these methods is as follows: graphical, analytic or classic, specific, numerical, dynamic planning, heuristic methods. The details for each one of these subdivisions are presented in [5,6]. Heuristic methods are suitable to solve such kind of problems. Some examples for these methods include Genetic Algorithm (GA) [7,8], Tabu Search (TS) [9], Particle Swarm Optimization (PSO) [10,11], Gravitational Search Algorithm (GSA) [12], Artificial Bee Colony (ABC) aided by Differential Evolution (DE) [13], and Seeker Optimization Algorithm (SOA) [14].

Recent advances in information technology, telecommunication systems, and smart grids developments lead to amazing progression in various areas of power systems operation. A review of the literature shows that one of the major achievements in this regard is increasing capability of parameters monitoring like voltage profile, transient power, active power losses in the network lines, the criterion of stability margin, etc. In a smart grid, Advanced Metering Infrastructure (AMI), and Phasor Measurement Units (PMU) are installed on substations to enhance grid visibility, and to optimize the reactive power distribution on a lower level [15,16].

An issue raised in smart grids is that the decisions required to improve operating conditions take longer due to an increase in the volume of communicated data between the sources of data and control centers [17]. Moreover, today's operation, at the level of the power grid, is centralized. It ends in congested information flow from the lower levels of the system (distribution and consumption levels) to the higher levels (control center of the system).

To reduce information exchange between different sections and resulted in congestions, as well as improving fault tolerance in the power systems, researchers posit layered structures to replace the

* Corresponding author.
E-mail address: mohamadreza-hashemi@shahroodut.ac.ir (M. Hashemi).
Peer review under responsibility of Karabuk University.

https://doi.org/10.1016/j.jestch.2019.03.003
2215-0986/

Nomenclature

Abbreviations

SoS	System Of Systems
ICS	Incident Command System
ORPD	Optimal Reactive Power Dispatch
GA	Genetic Algorithm
TS	Tabu Search
PSO	Particle Swarm Optimization
GSA	Gravitational Search Algorithm
DE	Differential Evolution
SOA	Seeker Optimization Algorithm
AMI	Advanced Metering Infrastructure
PMU	Phasor Measurement Units
SCADA	Supervisory Control and Data Acquisition
EMS	Energy Management System
DORPC	Decentralized Optimal Reactive Power Control
JADE	Java Agent Development Framework
DGs	Distributed Generation
MINLP	Mixed Integer Nonlinear Programming
GAMS	General Algebraic Modeling System
DR	Demand Response

Symbols

x	represents decision variables for *ACT* on level $N+1$
$f(x)$	objective function of problem for *ACT* on level $N+1$
$h(x)$	equality constraints for *ACT* on level $N+1$
$g(x)$	inequality constraints for *ACT* on level $N+1$
y	represents decision variables for *ACT* on level N
$f(y)$	objective function of problem for *ACT* on level N
$h(y)$	equality constraints for *ACT* on level N
$g(y)$	inequality constraints for *ACT* on level N
$\tilde{x}$	local variables belong to *acts* on levels $N+1$
$\tilde{y}$	local variables belong to *acts* on levels N
z	common variable
λ	an objective variable sent from *ACT* on level $N+1$ to *ACT* on level N
γ	response variable sent from *ACT* on level N to *ACT* on level $N+1$
c	the difference between objective variable and Response variable
$\pi(c)$	penalty function
P_L, Q_L	power demanded by ACT_j on level N and supplied by level $N+1$ in the optimization problem of ACT_j
P_E, Q_E	power generated by the *ACT* on level $N+1$ supplied to *ACT* on level N in the optimization problem of the *ACT* on level $N+1$
N_A	number of *ACTs* on level N connected to an *ACTs* on level $N+1$
o	Hadamard coefficient (multiplication of relevant derivations of both matrices)
α_j	the coefficient of linear expression
β_j	coefficient of second order expression
ε_1	stop criterion of the interloop
ε_2	stop criterion of the exterior loop
$P^*_{E,j}, Q^*_{E,j}$	target variables of ACT_j on level N received from the *ACT* on level $N+1$
$P^*_{L,j}, Q^*_{L,j}$	target variables of ACT_j on level $N+1$ received from the *ACT* on level N
$QB^{j,N}_b$	reactive power generated by b^{th} capacitor bank related to the ACT_j on level N
$QG^{j,N}_g$	reactive power generated by g^{th} DG related to the ACT_j on level N
$Loss^N_j$	active power losses of the *ACTj* on level N
N_b	number of capacitor banks related to each ACT
N_g	number of DGs related to each ACT
ω	index for inner loop iteration
k	index for outer exterior iteration
$PG(i)$	active power generated by generator unit installed on the i^{th} bus (kW)
$QG(i)$	reactive power generated by generator unit installed on the i^{th} bus (kVAr)
$PL(i)$	active power consumed by a load connected to the i^{th} bus (kW)
$QL(i)$	reactive power consumed by a load connected to the i^{th} bus (kVAr)
$QBK(i)$	reactive power generated by capacitor bank installed on the i^{th} bus (kVAr)
$\theta(i,j)$	angle difference of bus i and j
$V(i)$	an amplitude voltage of i^{th} bus (pu)
$G(i,j)$	the conductance of line between bus i and j
$B(i,j)$	susceptance of the line between bus i and j
$\overline{PG(i)}$	maximum active power generation of generation unit installed on the i^{th} bus (kW)
$\underline{PG(i)}$	minimum active power generation of generation unit installed on the i^{th} bus (kW)
$\overline{QG(i)}$	maximum reactive power generation of generation unit installed on the i^{th} bus (kVAr)
$\underline{QG(i)}$	minimum reactive power generation of generation unit installed on the i^{th} bus (kVAr)
$\overline{V(i)}$	the maximum voltage of bus i
$\underline{V(i)}$	the minimum voltage of bus i
$S(i,j)$	apparent power flowing in line between bus i and j
$\overline{S(i,j)}$	maximum allowable apparent power flowing in line between bus i and j
M	integer variable
$QBKS(i)$	step capacity of bank capacitor installed on the i^{th} bus (kVAr)

hierarchical structure of Supervisory Control and Data Acquisition (SCADA) [18]. The merit of stratified structure over SCADA structure is control and decision-making capabilities at lower levels (e.g., sub-transmission and distribution networks) so that no communication is needed with the higher levels unless in an emergency. To this end, information models to convert the centralized control of voltage and reactive power to local one are investigated. In [19], the architecture of a data center is recognized as an Energy Management System (EMS). It is located on the upper part of a hierarchy composed of several information layers and the relays allocated on the feeder of the distribution substations are considered as the boundary between the levels.

A Decentralized Optimal Reactive Power Control (DORPC) scheme in smart grids is presented in [19]. The proposed methodology is developed based on a Holonic architecture which is capable of combining both autonomous and cooperative behaviors efficiently to attain the system goals. Such capabilities would considerably alleviate the concerns associated with the centralized approaches [19]. The Holonic architecture has some interesting features by which the objective functions of the ORPD could be optimized through a timely proposed strategy [20]. In [21] a new framework is introduced to develop a coupled active and reactive market in distribution networks. Distributed Energy Resources (DERs) such as synchronous machine–based distributed

Please cite this article as: M. Hashemi and M. H. Zarif, A novel two-stage distributed structure for reactive power control, Engineering Science and Technology, an International Journal, https://doi.org/10.1016/j.jestch.2019.03.003

generations and wind turbines offer their active and reactive powers to the proposed market. For the considered DERs, multicomponent reactive power bidding structures are introduced based on their capability curves. Also, the hourly speed variations of wind turbines are considered in the proposed model. In [22], an appropriate testbed is developed to validate the scheme in a realistic setting by linking MATLAB and Java Agent Development Framework (JADE) platforms to each other. Also, a Lagrangian Relaxation (LR) method based on the decomposition algorithm is used in the optimization process and adapting this method for the proposed distributed structure.

In [18] a new structure has been introduced to control loads in a distribution grid in which active and reactive loads are used as a source to reduce the grid operation problems. In this model, the centralized structure of the protective relays is integrated into the proposed control system. This structure is a combination of two smart structures represented in [23,24]. In the model presented by Granadda, it is required to zone various sections of power systems to make them autonomous, based on boundary variables for each region and linking lines [25]. In this model, it is assumed that some generators supply the same boundary variables (voltage, active and reactive power in interconnecting lines). Based on the above multi-regional model, a centralized system is converted into a multi-regional centralized one.

It should be noted that, in this model, each region requires a generator to supply the power for the transmission lines. The architecture presented in [26], enables the DERs to function as backups for static and dynamic voltage support of connected distribution networks. This control structure is employed in many problems and issues emanated from DERs at the distribution level, e.g., operation in the islanding mode, implementation of the electricity market, protective schemes, etc. Ref. [27] proposes a distributed multi-agent system based on optimal reactive control to improve energy efficiency and voltage profile in power grids in various operating conditions.

The present paper introduces a control structure, based on the System of Systems (SoS), in which agents at various levels are in charge of the control and management of reactive power and control equipment. The assumed agents are capable of managing the reactive power flow in grid lines by adjusting the control variables. The system should be managed with no violation of network constraints and should always be met. Each one of the agents in the proposed SoS structure communicates with each other through the communication infrastructure. The information exchanged among various agents of the proposed structure is comprised of the active and reactive power of lines common among agents. The present paper aims to reduce the total cost including the active power loss cost, the cost of reactive power purchased from generators and capacitor banks, based on prices offered in a restructured environment.

The main contributions of the proposed method are as follows:

- Proposing a hierarchical distributed structure based on SoS framework which has a more flexibility and fault tolerance.
- Proposing a new method for power system partitioning approach based on graph concept.
- Using a two-step optimization method based on the optimization process and adapting this method for the proposed distributed structure.
- Developing an appropriate testbed to validate the scheme in a realistic setting by linking MATLAB to each other.

The rest of the paper is organized as follows. Section 2 presents the proposed structure along with relevant equations and grid constraints. Section 3 contains the results obtained from simulations and analyses. The final section is devoted to conclusions.

2. Proposed structure

According to the literature and papers presented in this regard, a hierarchical distributed framework is presented for the ORPD problem in power grids. This framework is based on a SoS structure [28]. The SoS refers to a set of heterogeneous systems that act autonomously based on their objectives. These systems communicate with another to ensure safe and reliable operation of the whole SoS set. In addition to the SoS structure, a novel approach for the power system partitioning based on graph concept. This method has been described in the next sub-section.

2.1. Power system partitioning

In this section, a novel method for partitioning of power systems has been presented. For this aim consider the power system an graph $G(V,E)$ with vertex set $V = \{v_1, v_2, \ldots, v_n\}$ and edge set E. The $e_{ij} = (v_i, v_j)$ shows the weight of an edge between v_i and v_j. The adjacency matrix of each graph has been illustrated as A. In the partitioning problem; the goal is to separate the main graph to K sub-graphs so that the total weight of the edges between the subgraphs is minimized, which is expressed as (1):

$$C(P) = \min\left[1_n^t A 1_n - trace(\Pi^t A \Pi)\right] \tag{1}$$

where $P = \{V_1, V_2, \ldots, V_K\}$ is the K-partition of V and $V_1, V_2, \ldots, V_K$ are the vertex set of each subgraph. Also 1_n is an n-vector with all entries equal to one. The $\Pi = [\pi_{vj}]$ is a matrix $n \times K$ dimension which π_{vj} is equal to:

$$\pi_{vj} = \begin{cases} 1 & v \in V_j \\ 0 & v \notin V_j \end{cases} \quad \forall v \in V, \quad j = \{1, 2, \ldots, K\} \tag{2}$$

The $trace(\Pi^t A \Pi)$ represents the sum of the diagonal elements of the $\Pi^t A \Pi$ matrix, Π is an orthogonal matrix, and $\| \Pi \|_F = \sqrt{n}$. The notation $\| . \|_F$ denotes the Frobenius norm, i.e., $\| \prod \|_F = \sqrt{trace(\prod' \prod)}$. One can show that an $n \times K$ matrix $\prod$ is a K-partition matrix if and only if each row of $\prod$ is a vector of the canonical basis of R^K. Since $1_n^t A 1_n$ is always a constant number, (1) can be rewritten as (3)

$$\begin{aligned} &C(P) = \max trace(\Pi^t A \Pi) \\ &s.t. \quad \pi_{vj} \in \{0,1\} \quad \forall v, j \\ &\quad \Pi \text{ orthogonal} \\ &\quad \| \Pi \|_F = \sqrt{n} \end{aligned} \tag{3}$$

For solving the partitioning problem (3), eigenvalues and eigenvectors of A have been utilized. If A is normalized so that the sum of each row is equal to one and $e_{ij} = e_{ji}$, then the biggest eigenvalue of A will equal to one. Let $\lambda_1 > \lambda_2, \ldots > \lambda_K$ be the largest eigenvalues of A and $u_1, u_2, \ldots, u_K$ the corresponding orthonormal eigenvectors. It is convenient to define:

$$\begin{aligned} D &= diag[\lambda_1, \lambda_2, \ldots, \lambda_K] \\ U &= [u_1, u_2, \ldots, u_K] \end{aligned} \tag{4}$$

where $U'U = I_{K \times K}$ and $AU = DU$. Since $\prod$ is an orthogonal matrix, therefore $trace(\Pi' \Pi) = n$, and since the largest eigenvalue is equal to one, it can be express:

$$trace(\Pi^t A \Pi) = \sum_{i=1}^{K} \pi_i^t A \pi_i \leqslant \sum_{i=1}^{K} \pi_i^t \pi_i = trace(\Pi^t \Pi) = n \tag{5}$$

To clarify the subject, suppose the graph of Fig. 1 is divided into two subgraphs in such a way that the objective function of (4) is realized.

The A and $1_n' A 1_n$ matrices for this graph will be:

Please cite this article as: M. Hashemi and M. H. Zarif, A novel two-stage distributed structure for reactive power control, Engineering Science and Technology, an International Journal, https://doi.org/10.1016/j.jestch.2019.03.003

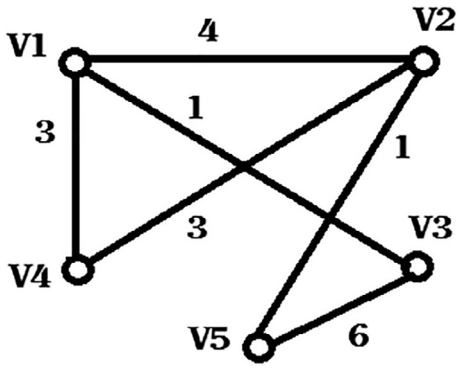

Fig. 1. A sample graph.

$$A = \begin{bmatrix} 8 & 4 & 1 & 3 & 0 \\ 4 & 8 & 0 & 3 & 1 \\ 1 & 0 & 7 & 0 & 6 \\ 3 & 3 & 0 & 6 & 0 \\ 0 & 1 & 6 & 0 & 7 \end{bmatrix} \quad 1_n^t A 1_n = 72 \tag{6}$$

Because of the simplicity of the graph, it is clear that the best partitioning will be at Table 1:

According to Table 1, the $\prod$ and $\Pi' A \Pi$ matrices are equal to:

$$\Pi = \begin{bmatrix} 1 & 0 \\ 1 & 0 \\ 0 & 1 \\ 1 & 0 \\ 0 & 1 \end{bmatrix} \quad \Pi^t A \Pi = \begin{bmatrix} 42 & 2 \\ 2 & 26 \end{bmatrix} \tag{7}$$

As can be seen, the non-diagonal elements of $\Pi^t A \Pi$ that are similar are equal to the sum of the weight of the edges interfacing two subgraphs. The value $trace(\Pi^t A \Pi)$ (68) is the closest value to $1_n^t A 1_n$ (72). Therefore, for the sample graph of Fig. 1, the (1) is realized.

A power system can be considered as a graph in which the buses and transmission lines are the vertex set and edge set of the graph. The size of each edge can be equal to the amplitude of the admittance, the active power, or reactive power flowing in the line. Therefore, the partition of the power system occurs in such a way that the sum of the amplitude of the admittance, or the active and reactive power passing through the lines between the sub-regions, is minimized. By doing this task, the power system is partitioned so that the voltage of the different areas will be as independent as possible.

2.2. The System of Systems (SoS)

There are different definitions for SoS. For instance, it is stated that the existence of SoS hinges on the dominance of 4 following features: (1) autonomous management and utilization, (2) geographical distribution, (3) novelty of behavior, and (4) evolutional development. SoSs are large distributed systems comprised of complex systems. Although there are similarities between the engineering of systems and SoSs, the research areas are different.

Table 1
Partitioning results of the sample graph.

	Vertices
Subgraph 1	V1, V2, V4
Subgraph 2	V3, V5

Engineering of traditional system aims to obtain the point of optimal operation of an isolated system, while in SoS the optimal operation of all grids is intended. Grids composed of interconnected systems cooperate to satisfy various goals and to guarantee that system constraints are met.

In a power system, based on SoS, the autonomous performance and decision making of each system should be guaranteed, while coordination of systems is taken into account. A centralized optimization which requires information from all parts of the grid does not seem to be an appropriate solution for the optimal point of performance. It is not easy to determine that point due to numerous control devices, generation, and consumption equipment. The information sent to the control center will be so voluminous which in turn requires an increase in the bandwidth of communication infrastructure because a lot of information should be sent to the control center at each moment. Meanwhile, this voluminous sent data can cause congestion at some points which makes online control of grid more troublesome. Moreover, the centralized mode increases the volume of data to be processed in the control center. This, in turn, necessitates powerful processors and optimization algorithms, and the volume of data increases the computation time. Last but not the least, centralized mode reduces the fault tolerance because losing a communication line with the upper level can void the control of the grid. It is less troublesome in a decentralized model than centralized ones. A SoS is defined as a set of several task-oriented and dedicated systems functioning in a single system. Its components have the following characteristics:

(1) Constituent systems put together their resources to form a more complicated system whose capability and performance are better than the sum of constituent systems.
(2) Whenever one of the constituent systems is disconnected from the whole system, its components can run the system based on tasks defined to achieve predetermined goals.

2.3. Optimal reactive power dispatch based on SoS

In the suggested framework, the power grid is categorized into several sets. Each set controls a section of the power grid. In restructured power systems, these sections can be the very Transmission System Operators (TSOs), and in ordinary ones, these sections can be planned by the system designers themselves. As a whole, by dividing the grid into several subdivisions, each subdivision is required to perform its ORPD operation independently from others.

Consequently, each section tries to minimize its objective through a set of control variables and based on relevant constraints. Since subdivisions communicate with each other at the boundary points, alteration in control variables of a subdivision may affect other subdivisions, as well. On the one hand, each subdivision solely has access to its information. On the other hand, system variables and parameters, like power flow, should match at boundary points. Therefore, two types of variables (objective and response) are defined in the proposed SoS. These two types of variables are exchanged between the subdivision and the central unit. A central control unit is contemplated in the proposed system which is merely in charge with coordination between subdivisions. This unit communicates the information between subdivisions and monitors their performance. Each subdivision submits its information to the central unit which dispatches it to other subdivisions if needed.

Each subdivision, according to information received from the central unit, solves its ORPD problem and sends its boundary variable to the central unit. The central unit receives the information sent by subdivisions and, if the difference among boundary variables is smaller than a given tolerance, it will announce the final

Please cite this article as: M. Hashemi and M. H. Zarif, A novel two-stage distributed structure for reactive power control, Engineering Science and Technology, an International Journal, https://doi.org/10.1016/j.jestch.2019.03.003

status to them. If the difference exceeds the allowed limit, the boundary values will be sent back to the corresponding subdivisions for adjustment. Each subdivision receives the boundary information of its neighboring subdivisions, then incorporates the difference between the previously announced boundary variable (from prior iteration) and the values calculated by neighboring subdivision and dispatched by the central unit into its objective function. The resultant value will be resent to the central unit. It should be mentioned that only boundary values will be sent to the central units. Once more, central units review the obtained variables and if required sends them back to the subdivisions.

Fig. 2 represents the schematic of the proposed design. The same procedure (as stated for transmission network and central unit) will be repeated for each subdivision of the second layer. Each subdivision is in turn divided into even smaller subdivisions until we come to the layer of actuators. In fact, this framework is a multi-layer hierarchical structure in which control is distributed and coordinated by supervision of an upper unit.

Compared to ordinary power systems, in the restructured type, power distribution networks will be active distribution networks due to the incorporation of DERs, responsive loads, and participation of private companies. As evident in Fig. 2, in a power grid, transmission of electricity and information is bi-directional. That is, information/electricity is transferred to the distribution network and vice versa. It makes an analysis of the system more complicated. In restructured systems, several operators are often defined. These operators are in charge with control and management of different sections of the grid. In new smart systems, these items can be considered as an agent and a smart control unit. In this paper, these operators (agents) are defined as *ACTs* and are indexed according to their levels. For instance, $ACT_{1,1}$ means agent number 1 on level 1. After defining *ACTs* as independent system regulators, the schemes for control and utilization of power systems can be designed and implemented based on an SoS framework.

Implementation of the SoS framework is challenging though, e.g., formulation of the optimization problem, evaluation and assessing the situation and decision making under various conditions, modeling economic issues, and competitive behavior of autonomous systems. Moreover, the information required to model the behavior of independent systems and the process of data exchange between systems should be determined and guaranteed. This paper addresses the ORPD problem in power systems based on an SoS framework. In this model, as it was stated before, *ACTs* are in charge of the operation of their regions. The Independent System Operator (ISO) is the highest *ACT* in this model, an autonomous system operator charged with the performance of transmission network. On the contrary, *ACTs* are operators of lower level independent systems using the distribution grid. Each *ACT* separately solves its ORPD problem based on the existing resources in the network, its topology and predicted loads.

An ordinary ORPD problem can be used for an independent system. Each *ACT* solves its ORPD separately to determine the optimal point of performance. It is noteworthy that on the lower level *ACTs*, several DERs units may have different owners (customers or distribution grid operators).

In addition to owning some of the units, the operator of the distribution grid can play the role of the regulator to manage and control DERs and equipment belonging to subscribers in solving the ORPD problem. As mentioned in Section 1, up to the now, various methods are proposed to solve ORPD problems. In this paper, a Mixed Integer Nonlinear Programming (MINLP) model is used to solve the ORPD problem for each independent system.

If there is no relation between *ACTs* on two consecutive levels, *ACTs* can solve their ORPD problems separately, and schedule their performance in different hours of the day. But, in this case, grids associated with different *ACTs* are interconnected, and the best point of performance for each of the grids affect the others. To model the communication between the systems in an OPRD

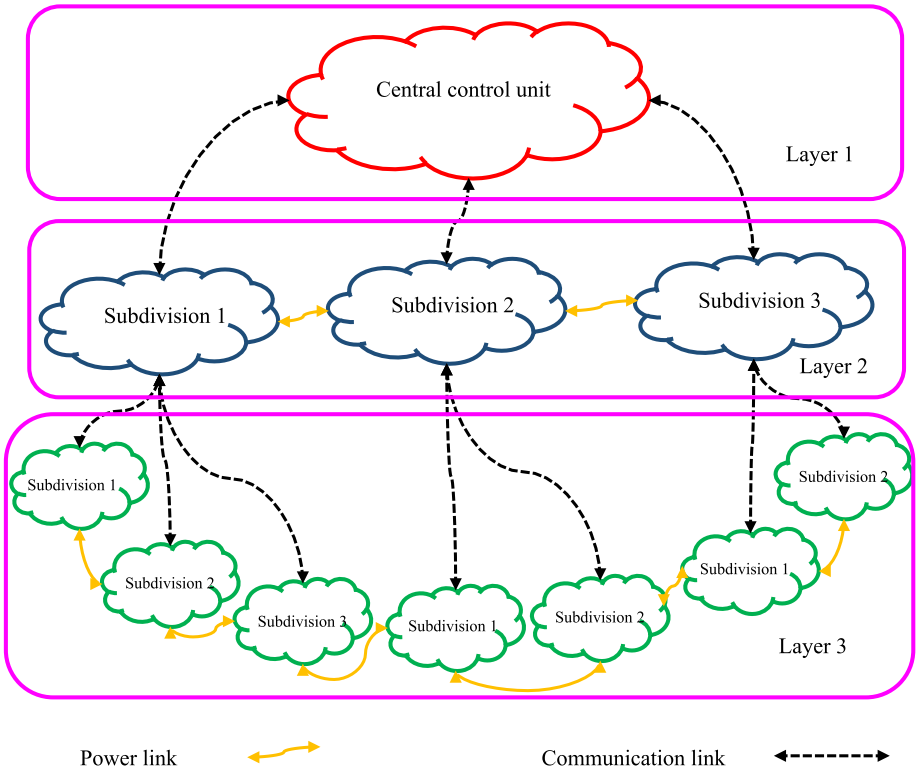

Fig. 2. Schematic representation of power systems as an SoS.

Please cite this article as: M. Hashemi and M. H. Zarif, A novel two-stage distributed structure for reactive power control, Engineering Science and Technology, an International Journal, https://doi.org/10.1016/j.jestch.2019.03.003

problem based on SoS, and finding the optimum point of performance for *ACTs*, a decentralized decision-making method is presented which conforms better to distributed technologies and participation of active distribution grids on the electricity market. A bi-level hierarchical optimization method can be used to implement decentralized decision making for an OPRD problem, based on SoS.

Fig. 3 shows an *ACT* of level *N* connected physically to another *ACT* on the level *N + 1*. Assume that (8) shows an overall ORPD problem for an *ACT* on the level *N + 1*:

$$\begin{aligned} &Min \quad f(x) \\ &s.t. \quad g(x) \leqslant 0 \\ &\quad\; h(x) = 0 \end{aligned} \tag{8}$$

The above problem can be similarly rewritten for an *ACT* on the level *N*:

$$\begin{aligned} &Min \quad f(y) \\ &s.t. \quad g(y) \leqslant 0 \\ &\quad\; h(y) = 0 \end{aligned} \tag{9}$$

Levels *N* and *N + 1* of the grid are connected through a power substation and share some variables. In this model, local variables are defined as $\tilde{x}$ and $\tilde{y}$ which belong to *ACTs* on levels *N + 1* and *N*, respectively. The common variables are defined with z which is common between two independent systems. Thus, Eqs. (8) and (9) are rewritten as follows:

$$\begin{aligned} &Min \quad f(\tilde{x},z) \\ &s.t. \quad g(\tilde{x},z) \leqslant 0 \\ &\quad\; h(\tilde{x},z) = 0 \end{aligned} \tag{10}$$

$$\begin{aligned} &Min \quad f(\tilde{y},z) \\ &s.t. \quad g(\tilde{y},z) \leqslant 0 \\ &\quad\; h(\tilde{y},z) = 0 \end{aligned} \tag{11}$$

Due to common variable *z*, Eqs. (10) and (11) cannot be solved separately. To analyze the above optimization problems independently, an SoS bi-level hierarchical framework is represented in Fig. 3, in which *ACTs* of levels *N + 1* and *N* are on the upper and the lower levels, respectively. Two different sets of variables are defined by common model variables and objective function. Then the constraints of each autonomous system are formulated. The first variable, λ, is called the objective variable as a vector of variables common between two systems sent from *ACT* on level *N + 1* to the *ACT* on level *N*. In fact, λ is sent from the upper level to the lower level. Response variable γ is the second vector variable of common variables sent from *ACT* level *N* to *ACT* level *N + 1*. According to the objective and response variables, the integrity constraint is defined as follows:

$$c = \lambda - \gamma = 0 \tag{12}$$

Constraint (12) should be taken into account in optimization problems of *ACTs* on both *N + 1* and *N* levels. The integrity constraints can be met using the penalty function. Hence, the local optimization problem of *ACTs* on levels *N + 1* and *N* are rewritten as Eqs. (13) and (14):

$$\begin{aligned} &Min \quad f(\tilde{x},z) + \pi(c) \\ &s.t. \quad g(\tilde{x},z) \leqslant 0 \\ &\quad\; h(\tilde{x},z) = 0 \\ &\quad\; \forall z \in \{\gamma,\lambda\} \end{aligned} \tag{13}$$

$$\begin{aligned} &Min \quad f(\tilde{y},z) + \pi(c) \\ &s.t. \quad g(\tilde{y},z) \leqslant 0 \\ &\quad\; h(\tilde{y},z) = 0 \\ &\quad\; \forall z \in \{\gamma,\lambda\} \end{aligned} \tag{14}$$

2.4. Method of modeling exchanged variables

In this section, the objective and response variables are determined as variables common between systems, based on the physical connection between two grids of different levels. As can be seen in Fig. 3, active and reactive powers exchanged through physical connection are identical with variables common between two independent systems. These variables of the ORPD problem interconnect the *ACTs* of levels *N + 1* and *N*. Assume that power of the *ACT* of level *N + 1* is transferred to the *ACT* of level *N*. The objective and response variables can be modeled as depicted in Fig. 3(c), where *ACT* of system on level *N + 1* is 1, and on level *N* equals 2. From the perspective of the *ACT* on level *N + 1*, the power flow in the common line is modeled as an assumed load fed by the *ACT* on levels *N + 1*.

Consequently, λ equals to assumed generation for the *ACTs* on level *N* and γ is the assumed load for *ACTs* on level *N + 1*. It should be mentioned that the assumed generation can be negative. That is, the ACT of level N delivers the power to the *ACT* of *N + 1*. It is the same for γ.

The power consumed by the *ACT* on level *N*, and power supplied by the *ACT* on level *N + 1* are defined in (15) as a part of optimization problem for the *ACT* on level *N*. The generated power by the *ACT* on level *N + 1* that sent to the *ACT* of level *N* for optimization problem of *ACT* on level *N + 1* is defined as (16).

$$\gamma = \{P_L, Q_L\} \tag{15}$$

$$\lambda = \{P_E, Q_E\} \tag{16}$$

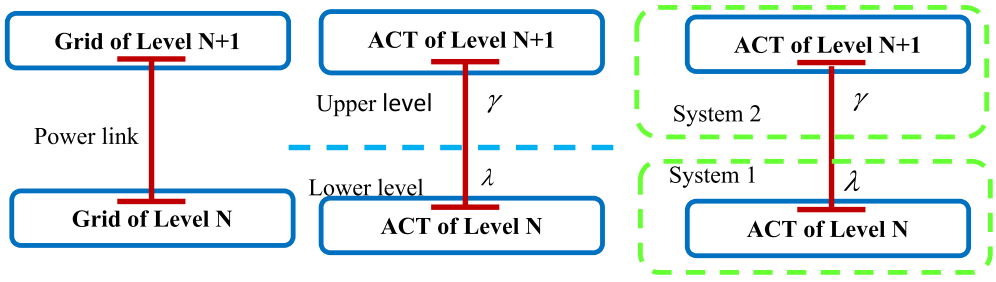

Fig. 3. (a) An *ACT* on level *N* which is physically connected to another *ACT* on the level *N + 1*. (b) A bi-level SoS structure. (c) Modeling variables.

Please cite this article as: M. Hashemi and M. H. Zarif, A novel two-stage distributed structure for reactive power control, Engineering Science and Technology, an International Journal, https://doi.org/10.1016/j.jestch.2019.03.003

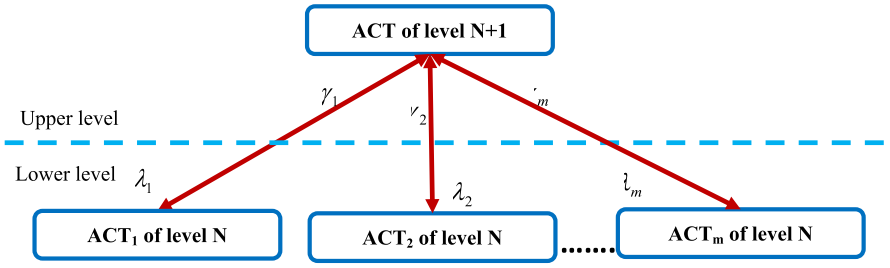

Fig. 4. Power system as bi-level hierarchical SoS.

When there are many *N* level grids connected to a grid on level *N + 1*, Fig. 3 evolves to Fig. 4. The only existing system on the higher level is the *ACT* of level *N + 1*, and all *N* level grids are on a lower level.

The *ACT* of level *N + 1* share variables with a great number of *N* level *ACTs*. The relevant optimization of (13) is rewritten as Eq. (17) which includes a penalty function to model integrity constraints between the *ACT* on level *N + 1*, and all *ACTs* on level *N*.

$$\begin{aligned} Min \quad & f(\tilde{x}, z_1, z_2, ..., z_j) + \pi(c_1, c_2, ..., c_j) \\ s.t. \quad & g(\tilde{x}, z_1, z_2, ..., z_j) \leqslant 0 \\ & h(\tilde{x}, z_1, z_2, ..., z_j) = 0 \\ & \forall_j = 1, 2, ..., N_A \\ & \forall z_j \in \left\{\lambda_j, \gamma_j\right\} \end{aligned} \tag{17}$$

Incorporating some time span and using a second order function to model penalty function π, the problem of optimizing *ACT* on level *N + 1* (17) is converted into (18), where symbol o represents the Hadamard coefficient (multiplication of relevant derivations of both matrices).

$$\begin{aligned} & Min \quad f(\tilde{x}, z_1, z_2, ..., z_j) \\ & + \sum_{j=1}^{N_A} \left(\alpha_j(\lambda_j - \gamma_j) - \| \beta_j o(\lambda_j - \gamma_j) \|_2^2\right) \\ & s.t. \quad g(\tilde{x}, z_1, z_2, ..., z_j) \leqslant 0 \\ & \quad h(\tilde{x}, z_1, z_2, ..., z_j) = 0 \\ & \quad \forall_j = 1, 2, ..., N_A \\ & \quad \forall z_j \in \left\{\lambda_j, \gamma_j\right\} \end{aligned} \tag{18}$$

Similarly, the problem of optimizing ACT_j on level *N* can be rewritten as (19):

$$\begin{aligned} & Min \quad f(\tilde{y}, z_j) \\ & + \left(\alpha_j(\lambda_j - \gamma_j) + \| \beta_j o(\lambda_j - \gamma_j) \|_2^2\right) \\ & s.t. \quad g(\tilde{y}, z_{jt}) \leqslant 0 \\ & \quad h(\tilde{y}, z_j) = 0 \\ & \quad \forall z_j \in \left\{\lambda_j, \gamma_j\right\} \end{aligned} \tag{19}$$

In (11) and (12) z_j, λ_j and γ_j are respectively the common, objective and response variables between the *ACT* of level *N + 1*, and ACT_j of level *N*. The penalty function includes two linear and second order terms. Parameters α_j and β_j are coefficients of linear and second-order expressions. These parameters are updated throughout the solution process. An important feature of the second-order penalty function is that this function is a convex second order curve. Thus, the problem can be easily solved using a second-order optimization method.

2.5. Control of common parameters

ORPD problems of autonomous systems including penalty functions, and objective/response variables are interrelated. This equation is established aiming to obtain the overall results of the power system. Consequently, the ORPD problem of relevant ACT_j on level *N* is demonstrated as follows:

$$Min \left[\begin{array}{c} \left[\sum_{b=1}^{N_B} QB_b^{j,N} \times CQB_b^{j,N} + \sum_{g=1}^{N_g} QG_g^{j,N} \times CQG_g^{j,N} + Loss_j^N \times C_{loss}\right] + \\ \left(\left(\alpha P_j(P_{E,j}^* - P_{L,j}) + \| \beta P_j o(P_{E,j}^* - P_{L,j}) \|_2^2\right) + \\ \left(\left(\alpha Q_j(Q_{E,j}^* - Q_{L,j}) + \| \beta Q_j o(Q_{E,j}^* - Q_{L,j}) \|_2^2\right) \end{array}\right] \tag{20}$$

The first expression of Eq. (20), is the objective function of ORPD problem of ACT_j on level *N*. In this paper, it includes the cost of reactive power generation by capacitor banks and DERs as well as losses cost. The second expression is the penalty function of common variables with the *ACT* on level *N + 1*. It should be mentioned that in penalty function, we need to determine the response variables $Q_{L,j}$ and $P_{L,j}$, but the value of the objective function $P_{E,j}^*$ is obtained from the *ACT* on level *N + 1*. Meanwhile, the usual ORPD constraints should be satisfied.

The ORPD problem (21) relates to the *ACT* of level *N + 1*. Response variables of *ACTs* on level N are received to model the penalty function. In this problem, $P_{E,j}$ is assumed as a vector of designing variables, while $P_{L,j}^*$ variables are assumed to be constant.

$$Min \left[\begin{array}{c} \left[\sum_{b=1}^{N_B} QB_b^{j,N} \times CQB_b^{j,N} + \sum_{g=1}^{N_g} QG_g^{j,N} \times CQG_g^{j,N} + Loss_j^{N+1} \times C_{loss}\right] + \\ \sum_{j=1}^{N_A} \left(\begin{array}{c} \left(\left(\alpha P_j(P_{E,j} - P_{L,j}^*) + \| \beta P_j o(P_{E,j} - P_{L,j}^*) \|_2^2\right) + \\ \left(\left(\alpha Q_j(Q_{E,j} - Q_{L,j}^*) + \| \beta Q_j o(Q_{E,j} - Q_{L,j}^*) \|_2^2\right) \end{array} \right) \end{array}\right] \tag{21}$$

Similarly, in Eq. (21), the first expression shows the objective function of the *ACT* on level *N + 1*, and the second expression is the penalty function of variables common with *ACTs* on level *N*.

2.5.1. Constraints

In the ORPD program of systems, the objective function is defined as (20) and (21), and constraints are expressed as below:

(A) Power flow equations

$$PG(i) - PL(i) = V(i) \sum_{j=1}^{N_i} V(j)(G(i,j)\cos\theta(i,j) + B(i,j)\sin\theta(i,j)) \tag{22}$$

Please cite this article as: M. Hashemi and M. H. Zarif, A novel two-stage distributed structure for reactive power control, Engineering Science and Technology, an International Journal, https://doi.org/10.1016/j.jestch.2019.03.003

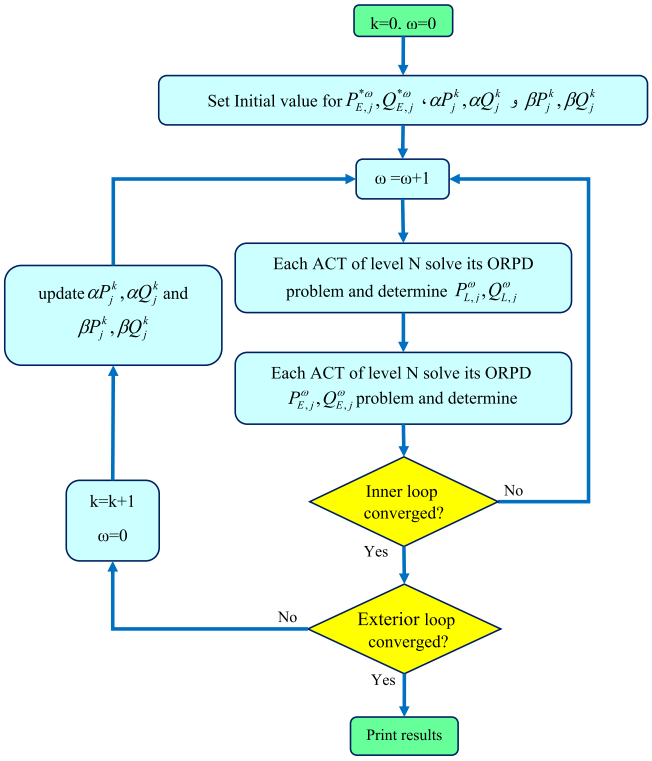

Fig. 5. Flowchart of the problem.

$$QG(i)+QBK(i)-QL(i)=V(i)\sum_{j=1}^{N_i}V(j)(B(i,j)\cos\theta(i,j)-G(i,j)\sin\theta(i,j)) \quad (23)$$

(B) Generator power limitation

$$\underline{PG(i)} \leqslant PG(i) \leqslant \overline{PG(i)} \quad (24)$$

$$\underline{QG(i)} \leqslant QG(i) \leqslant \overline{QG(i)} \quad (25)$$

(C) Operational constraints

$$\underline{V(i)} \leqslant V(i) \leqslant \overline{V(i)} \quad (26)$$

$$S(i,j) \leqslant \overline{S(i,j)} \quad (27)$$

(D) Capacitor bank constraints

$$QBK(i) = M \times QBKS(i) \quad (28)$$

2.6. Progress procedure of the presented method

Fig. 5 shows the suggested solution method which results in scheduling control equipment of *ACTs* on levels *N + 1* and *N*. This algorithm has two repetitive loops as follows:

Step 1: Repetition indices of ω and k which relate to interior and exterior loops are assumed to be zero, and the initial values of variables $P^{*\omega}_{Ej}, Q^{*\omega}_{Ej}$ are determined, as well as variables $\beta P^k_j, \beta Q^k_j$ $\alpha P^k_j, \alpha Q^k_j$.

Step 2: Set $\omega = \omega + 1$ and solve the ORPD problem for each *ACT* of level *N*, based on $P^{\omega}_{Lj}, Q^{\omega}_{Lj}$ as design variables. On this step, variables $P^{\omega}_{Lj}, Q^{\omega}_{Lj}$ are determined based on their previous repetition $(P^{\omega-1}_{Lj}, Q^{\omega-1}_{Lj})$.

Step 3: The ORPD problem for the *ACT* on level *N + 1* is solved based on $P^{\omega}_{Ej}, Q^{\omega}_{Ej}$ as designing variables and the values of $P^{*\omega}_{Lj}, Q^{*\omega}_{Lj}$ as computed in the second step.

Step 4: Using (29) and (30), the convergence of interior loop is investigated. If the condition is not met, there is a return to step 2 to begin the next iteration. Otherwise, we proceed to step 5.

$$P^{\omega}_{Ej} - P^{\omega-1}_{Lj} \leqslant \varepsilon_1 \quad \text{and} \quad Q^{\omega}_{Ej} - Q^{\omega-1}_{Lj} \leqslant \varepsilon_1 \quad \forall_j \quad (29)$$

$$P^{\omega}_{Lj} - P^{\omega-1}_{Lj} \leqslant \varepsilon_1 \quad \text{and} \quad Q^{\omega}_{Lj} - Q^{\omega-1}_{Lj} \leqslant \varepsilon_1 \quad \forall_j \quad (30)$$

Step 5: Constraints (31) is investigated as the stop criterion of the exterior loop. If the constraints are not met, there is a move to step 6. Otherwise, the optimization results converge, and the solving process comes to an end.

$$P^{\omega}_{Ej} - P^{\omega}_{Lj} \leqslant \varepsilon_2 \quad and \quad Q^{\omega}_{Ej} - Q^{\omega}_{Lj} \leqslant \varepsilon_2 \quad \forall_j \quad (31)$$

Step 6: We assume $k = k + 1$ and the values for coefficients $\beta P^k_j, \beta Q^k_j$ $\alpha P^k_j, \alpha Q^k_j$ are updated based on Eqs. (32)–(35):

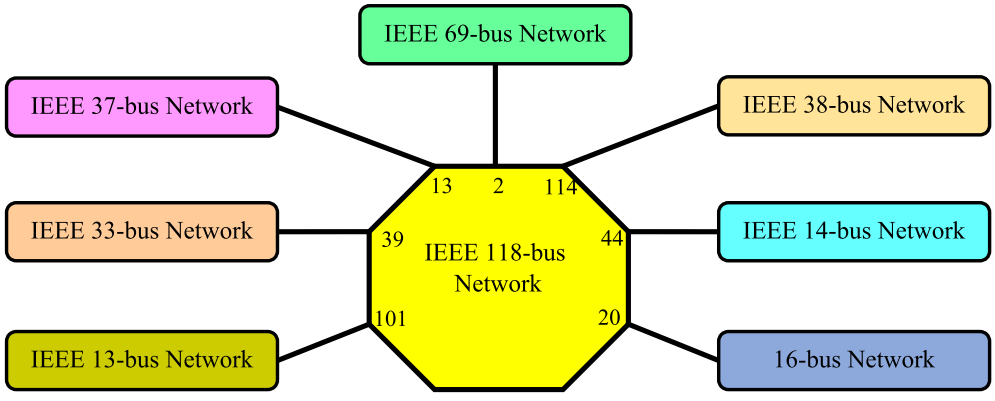

Fig. 6. The test system.

Please cite this article as: M. Hashemi and M. H. Zarif, A novel two-stage distributed structure for reactive power control, Engineering Science and Technology, an International Journal, https://doi.org/10.1016/j.jestch.2019.03.003

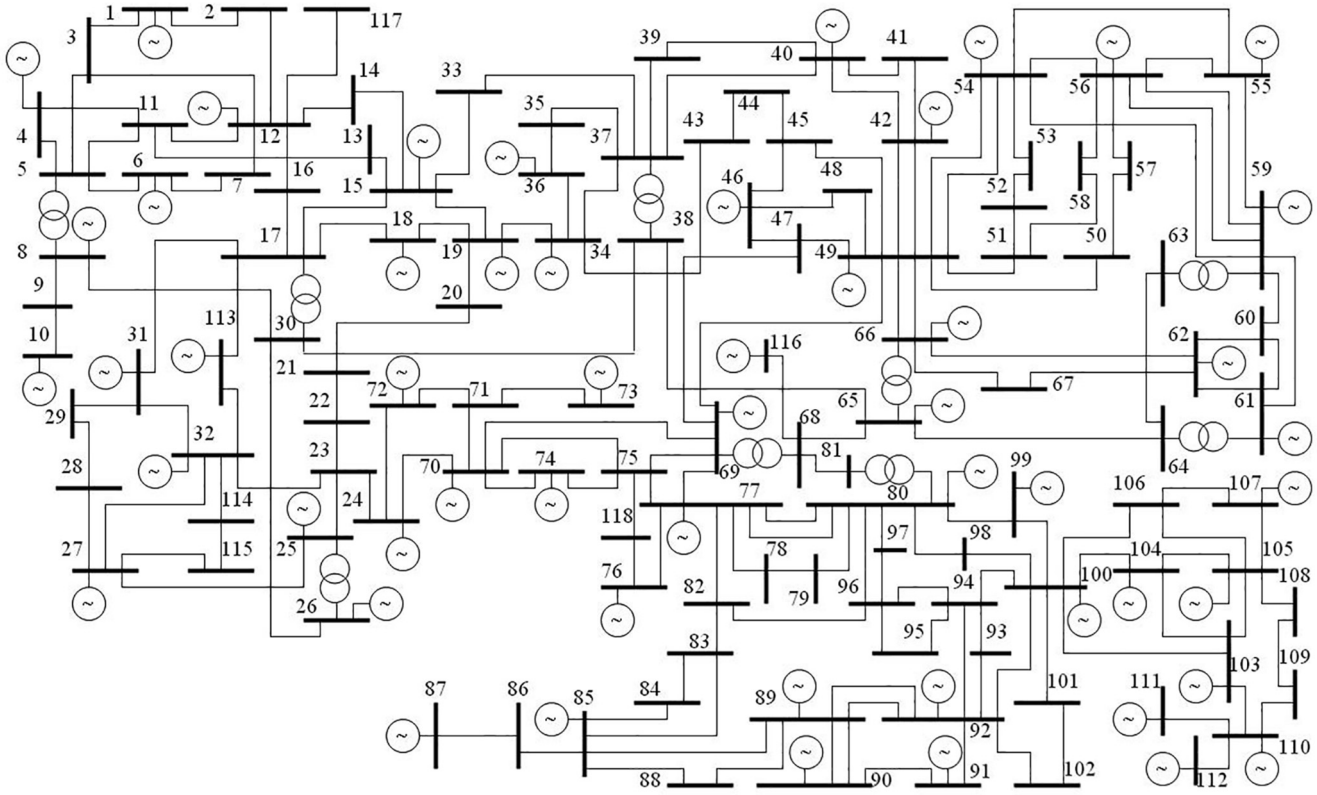

Fig. 7. The initial single diagram of the IEEE 118-bus test system before partitioning approach.

$$\alpha P_j^{(k+1)} = \alpha P_j^{(k)} + 2(\beta P_j^{(k)})^2 (P_{E,j}^{\omega} - P_{L,j}^{\omega}) \tag{32}$$

$$\beta P_j^{(k+1)} = \Delta \beta P_j^{(k)} \tag{33}$$

$$\alpha Q_j^{(k+1)} = \alpha Q_j^{(k)} + 2(\beta Q_j^{(k)})^2 (Q_{E,j}^{\omega} - Q_{L,j}^{\omega}) \tag{34}$$

$$\beta Q_j^{(k+1)} = \Delta \beta Q_j^{(k)} \tag{35}$$

where the coefficient Δ must be equal or larger than 1 to obtain converged optimization results. This updating procedure of Lagrangian coefficients is attested in [29] for convergence to an optimum result.

Step 7: We set $P_{E,j}^{*0} = P_{E,j}^{*\omega}, Q_{E,j}^{*0} = Q_{E,j}^{*\omega} \forall j,\ \omega = 0$, and return to step 2.

It should be mentioned that in the loop of internal iteration of the algorithm, the coefficients of penalty are constant and only $P_{E,j}$ '$P_{L,j}$' $Q_{E,j}$ and $Q_{L,j}$ should be updated. Such a method helps the algorithm achieve an answer with reasonable precision, especially when our guess for initial values of common variables is not accurate.

3. Simulation results

In this paper, the IEEE 118-bus network is considered as the case study [30]. The presented method is applied to this network to assess its performance. To investigate the performance of the proposed structure, two other methods (a distributed method based on the Incident Command System (ICS) [18], the centralized control method) have been simulated, and their results have been compared with the proposed ones.

The proposed method has been applied on the IEEE 118-bus test systems as transmission network connected to the 7 Active Distribution Grids (ADGs) including IEEE 14-bus [31], IEEE 33-bus [31], IEEE 37-bus [32], IEEE 38-bus [33], IEEE 69-bus [33], 16-bus [32] and 13-bus [34]. The schematic of the test system is shown in Fig. 6. For a better illustration of the proposed method and its results, the single diagram of the IEEE 118-bus test system has been shown in Fig. 7. This diagram the initial status of the IEEE 118-bus when the proposed partitioning approach (first stage) has been not applied. The IEEE 118-bus test has 19 generation units, 35 synchronous condensers, 177 lines, 9 transformers, and

Table 2
Location and size of capacitors.

Network	Bus	Size (kVA)	Network	Bus	Size (kVA)
37-bus system	13	600	33-bus system	12	60
37-bus system	34	300	33-bus system	9	60
37-bus system	35	300	33-bus system	30	100
37-bus system	31	250	33-bus system	33	150
37-bus system	23	200	33-bus system	27	80
37-bus system	25	200	33-bus system	25	80
37-bus system	29	300	33-bus system	22	50
16-bus system	6	700	33-bus system	7	50
16-bus system	12	600	33-bus system	18	150
16-bus system	16	300	33-bus system	15	100
16-bus system	4	250	69-bus system	43	50
14-bus system	9	100	69-bus system	36	50
14-bus system	7	100	69-bus system	21	60
14-bus system	3	100	69-bus system	17	60
14-bus system	4	50	69-bus system	15	50
38-bus system	18	50	69-bus system	9	50
38-bus system	22	50	69-bus system	16	50
38-bus system	12	60	13-bus system	611	100
38-bus system	25	60	13-bus system	680	100
38-bus system	33	50	13-bus system	675	100

Please cite this article as: M. Hashemi and M. H. Zarif, A novel two-stage distributed structure for reactive power control, Engineering Science and Technology, an International Journal, https://doi.org/10.1016/j.jestch.2019.03.003

Table 3
Location and size of DERs.

type	Network	Bus	Size (kW)	type	Network	Bus	Size (kW)
PV	37-bus system	36	250	WT	33-bus system	25	250
PV	37-bus system	31	300	PV	33-bus system	22	200
MT	37-bus system	5	250	MT	33-bus system	29	350
WT	37-bus system	21	300	WT	33-bus system	33	350
MT	37-bus system	30	600	PV	33-bus system	18	350
WT	37-bus system	15	100	PV	38-bus system	17	250
PV	16-bus system	15	250	WT	38-bus system	36	300
PV	16-bus system	11	200	WT	38-bus system	33	250
WT	16-bus system	6	300	PV	69-bus system	40	250
PV	14-bus system	13	100	MT	69-bus system	69	300
WT	14-bus system	4	100	WT	69-bus system	14	300
PV	13-bus system	675	100	WT	69-bus system	63	250

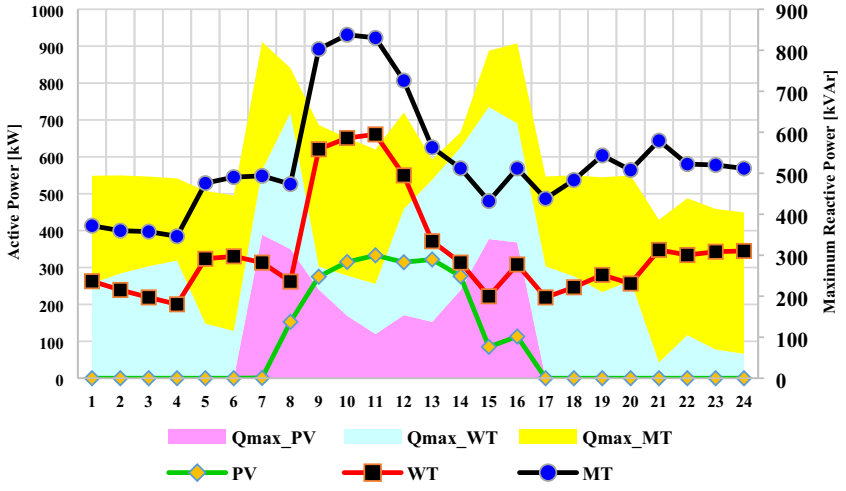

91 loads. The all needed data for different networks have been given from mentioned references.

The capacity and location of capacitor banks and DERs for each ADG has been given in Tables 2 and 3, respectively. It is assumed that all capacitor banks have 20 steps. Three DERs have been considered in the ADGs including photovoltaic units (PVs), Wind turbines (WTs) and Micro Turbines (MTs). The active power of PV and WT units depend on solar insolation and wind speed, respectively. Practically, there are several constraints on the reactive power production by DERs. In facts, the maximum reactive power capacity of DERs can be obtained by A1 in Appendix.

It is necessary to say that a DER would be turned on if it can produce active power. Otherwise, it will be turned off. Thus, if the active power of a DER is zero, its reactive power capacity will be

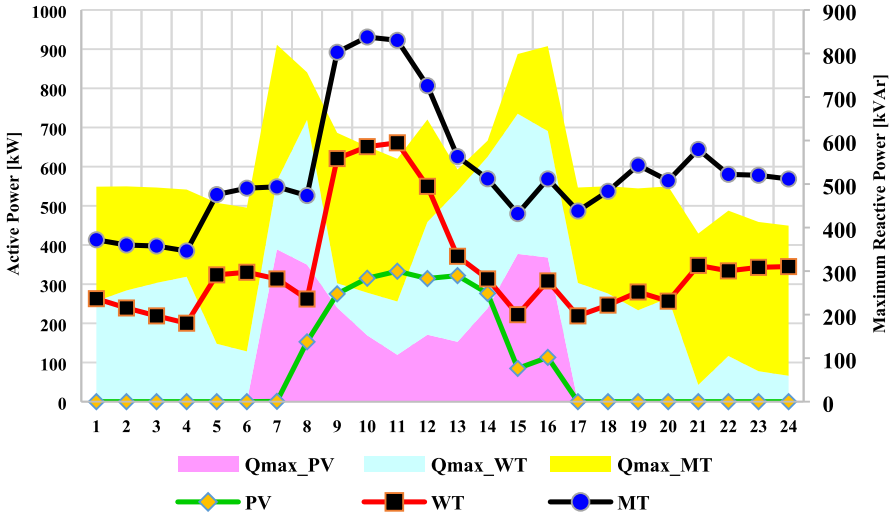

Fig. 8. DERs active power production and their maximum capacity for reactive power production.

Please cite this article as: M. Hashemi and M. H. Zarif, A novel two-stage distributed structure for reactive power control, Engineering Science and Technology, an International Journal, https://doi.org/10.1016/j.jestch.2019.03.003

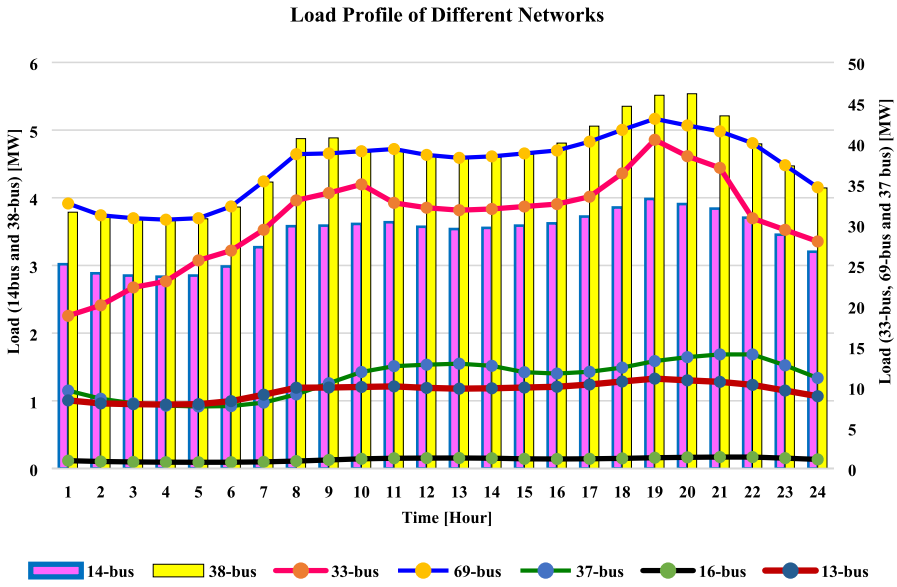

Fig. 9. The load profile of ADGs.

zero. This point will be important for PV units in hours that solar insolation is not available. It is assumed that all DERs in ADGs have the same pattern for solar insolation and wind speed. Therefore, their active power production is different in a coefficient depending on their capacity. Fig. 8 shows the active power output of typical PV, WT and MT units installed in the IEEE 33-bus ADG [32]. Also, the maximum reactive power capacity of these units has been illustrated in Fig. 8.

The investigated methods have been applied for a 24-hour period of time. The load profile of ADGs has been shown in Fig. 9. All calculations are performed through GAMS software package. To solve the proposed model OQNLP solver is employed.

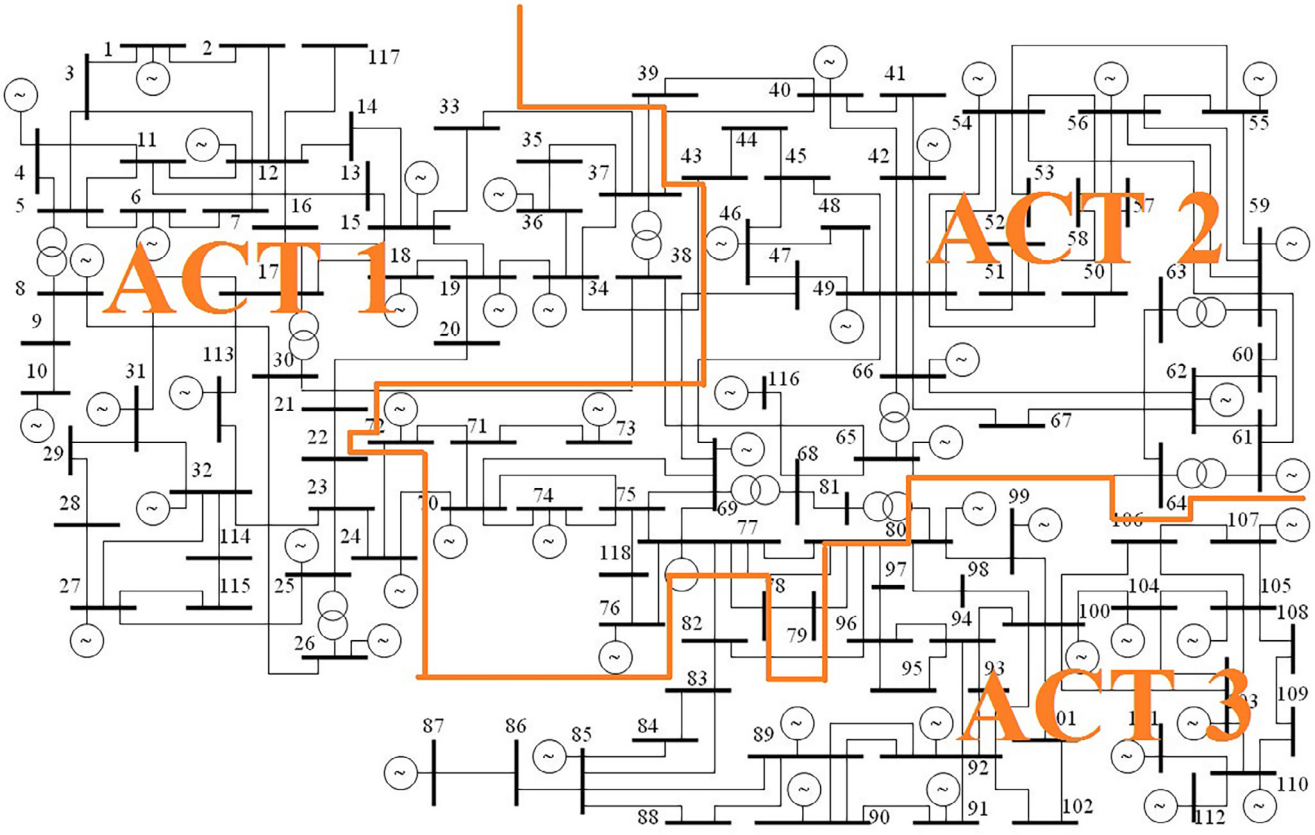

Fig. 10. The single diagram of the IEEE 118-bus test system after partitioning.

Please cite this article as: M. Hashemi and M. H. Zarif, A novel two-stage distributed structure for reactive power control, Engineering Science and Technology, an International Journal, https://doi.org/10.1016/j.jestch.2019.03.003

3.1. Simulation results

3.1.1. Results of the first stage (partitioning stage)

The proposed partitioning approach has been applied to the IEEE 118-bus test system based on the (1)–(5). The reactive power of transmission lines is considered as the partitioning criterion. The obtained the single diagram of the IEEE 118-bus system based on the proposed partitioning method, has been illustrated in Fig. 10. As can be seen, the whole of the system is divided into three parts.

3.1.2. Results of the second stage (SoS method)

The ORPD problem is solved by three structures to obtain the optimal point of system performance. As mentioned in Section 2, the cost of reactive power purchased from capacitor banks and DERs as well as losses cost is considered as an objective function of each system in the SoS structure. According to the concept of SoS, ADGs can be modeled as independent systems. The active and reactive powers transmitted between upstream transmission grid (the *ACT* of level $N+1$) and distribution grids (the *ACT* of level N) are considered as exchanged boundary variables. The initial values of parameters are assumed to be as follows:

$$\alpha P_j^0 = \alpha Q_j^0 = \beta P_j^0 = \beta Q_j^0 = 1$$

The detail of the obtained results for IEEE 33-bus network has been presented as a typical ADG. The six capacitors behavior of this ADG has been shown in Fig. 11. The reactive power production of three DERs of this ADG has been illustrated in Fig. 12. According to the PV unit output, it can be shown that the reactive power production is zero in hours that PV unit is turned off. Also in midday hours, the reactive power has been reduced due to an increase in active power production and capacity constraint mentioned in A1. The sum of the voltage deviation of buses and active power loss has been presented in Figs. 13 and 14, respectively. As can be seen, the proposed method leads to lower active power losses and voltage deviation. These figures show that the SoS based framework has more capability of reactive power control. The profile voltage of this ADG is presented in Fig. 15. One can be seen that all voltages are in the acceptable voltage range (0.95–1.05 pu) and there is no violation of voltage parameter.

The time computation and Fault Tolerance (FI) are two other factors to evaluate the performance of the proposed method. The time computation is related to the time of simulation. The fault-tolerance is also an important requirement, especially when the management nodes increase. To achieve the needed reliability and availability, it is needed fault-tolerant control structure.

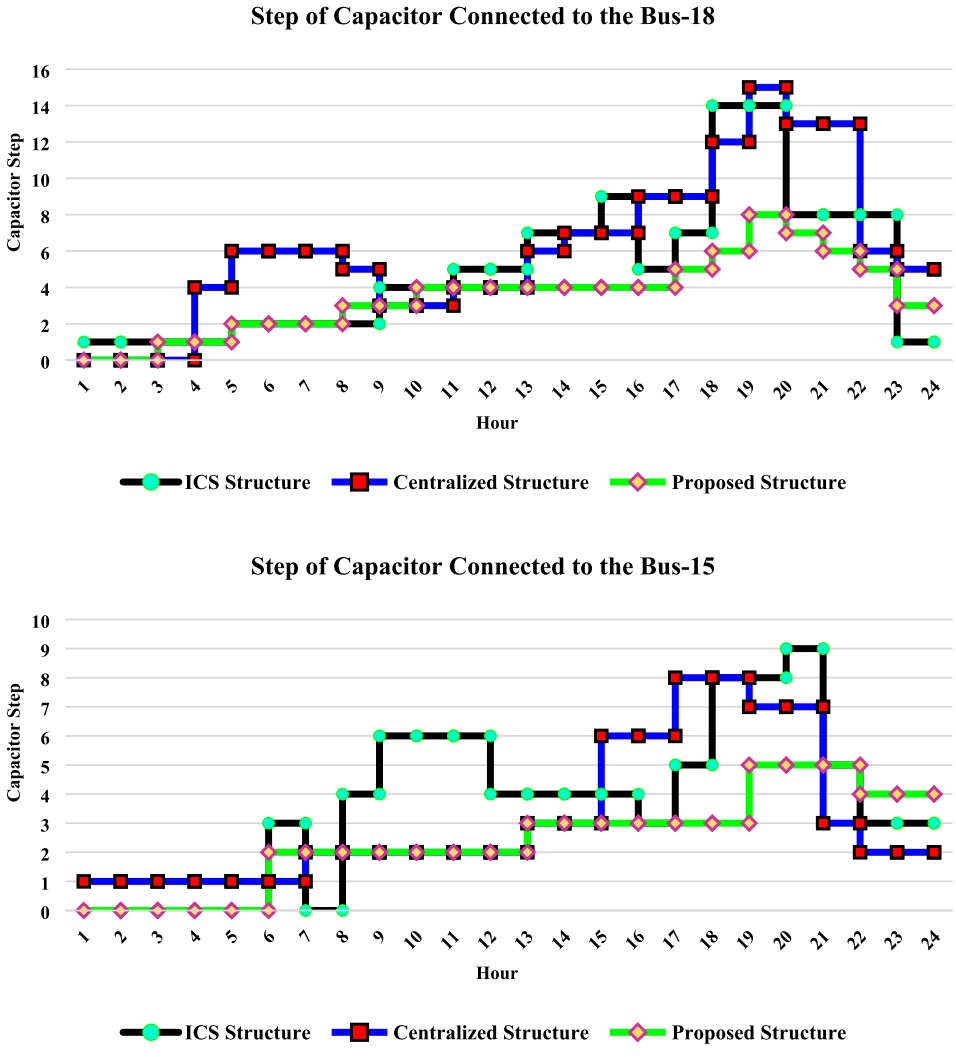

Fig. 11. Capacitor steps of IEEE-33 bus ADG for a 24-hour period of time.

Please cite this article as: M. Hashemi and M. H. Zarif, A novel two-stage distributed structure for reactive power control, Engineering Science and Technology, an International Journal, https://doi.org/10.1016/j.jestch.2019.03.003

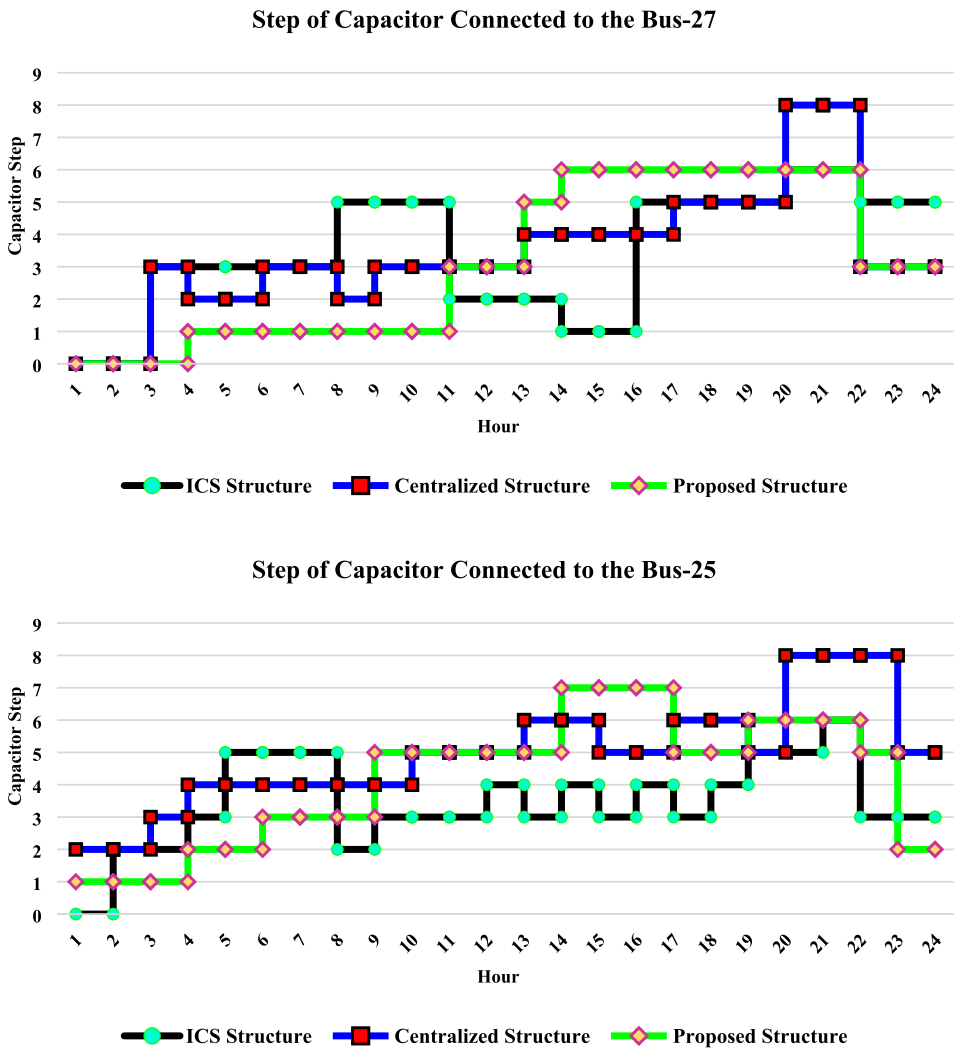

Fig. 11 (*continued*)

The method can tolerate faults by detecting failures and isolate defect modules so that the rest of the system can operate correctly. Several formulas have been defined for this index. In this paper, it is used from formulas presented in [35] for evaluation. They are given in Appendix as A2 and A3 for centralized and decentralized structures. The FI of three structures and their computational time have been given in Figs. 16 and 17, respectively. As can be seen, the centralized framework is much less fault-tolerant. This mater is related to its structure where all the agents are controlled by a unique supervisory agent, and its failure leads to overall failure. However, in the proposed method, the lower layers can manage themselves, even if the higher agent is failed. The less value related to the SoS framework refers to its dynamism feature. In fact, if an agent in a specific layer is lost, its sub-agent can be managed by the neighboring higher layer agent. Thus, the FI index of the framework increases.

4. Conclusion

This paper proposes a distributed hierarchical framework for ORPD in power systems based on SoS. In this structure, the power system is comprised of several layers. On each layer, some agents are in charge with optimal distribution of reactive power in the relevant section. Boundary variable is exchanged for control and coordination. The proposed method is simulated on the IEEE 118-bus power grid with seven active distribution grids. Different aspects of the obtained results are compared to the results of two other competing methods, i.e., a decentralized method based on ICS structure and a centralized method. The comparison approves that proposed method is appropriate for obtaining the optimum answer.

Moreover, the calculation volume and time are reduced in the proposed method, since the grid is locally controlled and managed.

Please cite this article as: M. Hashemi and M. H. Zarif, A novel two-stage distributed structure for reactive power control, Engineering Science and Technology, an International Journal, https://doi.org/10.1016/j.jestch.2019.03.003

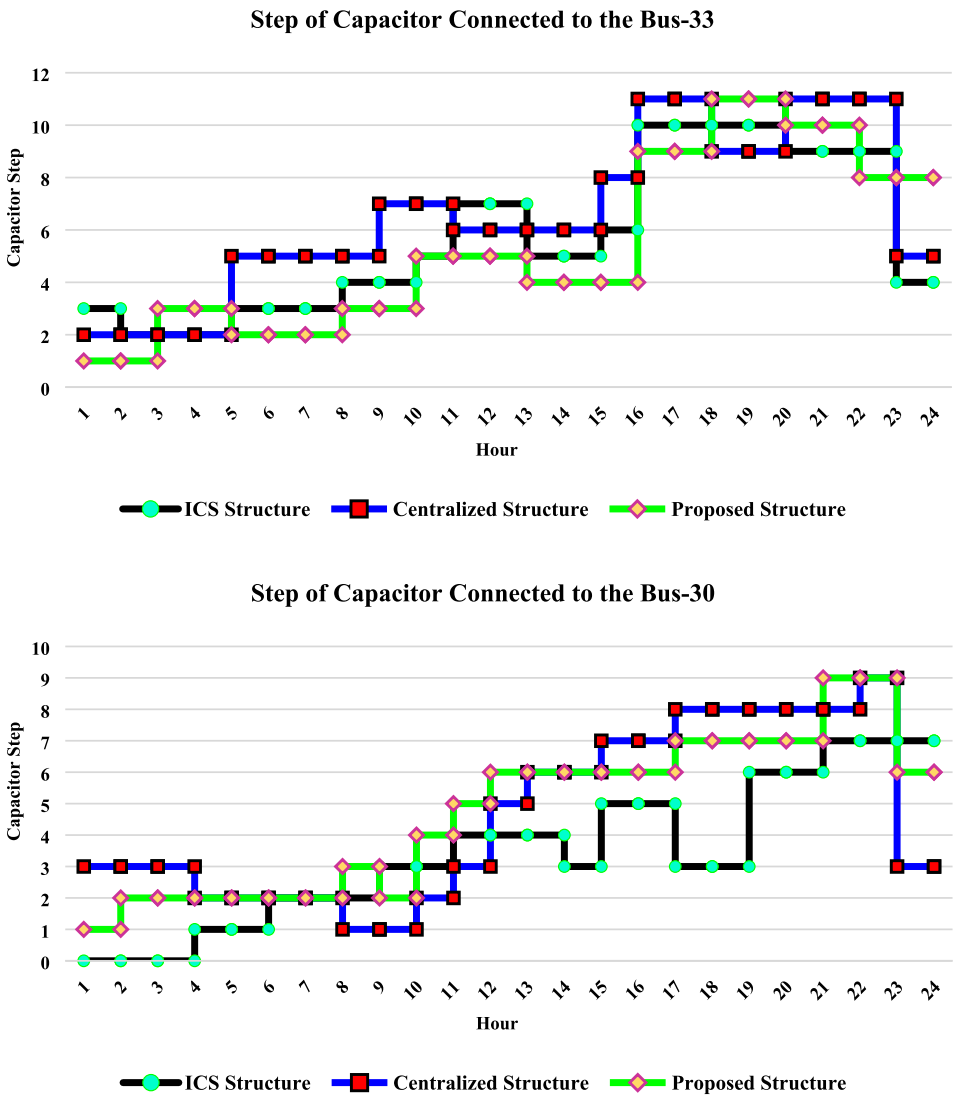

Fig. 11 (*continued*)

This result in a reduction of data sent to the control center, improvement of fault tolerance, enhancement of reliability and boosting decision speed.

Meanwhile, the power system is a complex system and based on the structure of restructured power systems, each section of the grid belongs to a specific agency, and it is not possible to have access to the whole grid information at once. The proposed method can satisfactorily take up the responsibility of control and distribution of reactive power. This structure can be employed to study other aspects of power grid utilization in the future, including energy management, load Demand Response (DR), etc.

Appendix A

The maximum reactive power capacity of DERs can be obtained by (A1)

$$QDG_i^{\max} = \sqrt{SDG_i^2 - PDG_i^2} \tag{A1}$$

Appendix B

The fault tolerance of centralized and decentralized structures can be calculated by (B1) and (B2) respectively.

$$FT_{centralized} = e^{-\left(\frac{A\times K\times EN^2}{T_0}+B\right)} \tag{B1}$$

where

A, B, and K Constants ($A = 0.1$, $B = 0.001$, $K = 0.1$)
EN Number of agents ($EN = 1000$)
T_0 The operation period of every EN ($T_0 = 3600$ s)

$$FT_{decentralized} = \frac{1}{w}\sum_{k=1}^{w-1}\left(1-\sum_{q=1}^{d^{k-1}}\binom{d^{k-1}}{q}\left(1-e^{-\left(\frac{A\times K\times d\times EN}{T_0}+B\right)}\right)^q \left(e^{-\left(\frac{A\times K\times d\times EN}{T_0}+B\right)}\right)^{d^{k-1}-q}\times\frac{q}{d^{k-1}}\right) + \frac{1}{w}\left(1-\sum_{q=1}^{d^{w-1}}\binom{d^{w-1}}{q}\left(1-e^{-\left(\frac{A_2K}{T_0}\left(\frac{EN}{d^{w-1}}\right)^2+B\right)}\right)^q\left(e^{-\left(\frac{A_2K}{T_0}\left(\frac{EN}{d^{w-1}}\right)^2+B\right)}\right)^{d^{h-1}-q}\times\frac{q}{d^{k-1}}\right) \tag{B2}$$

where

w Number of layers
d^{k-1} Number of ACTs (relays in ICS framework) in the k^{th} layer ($d = 5$ in SoS framework and $d = 3$ in ICS framework)

Please cite this article as: M. Hashemi and M. H. Zarif, A novel two-stage distributed structure for reactive power control, Engineering Science and Technology, an International Journal, https://doi.org/10.1016/j.jestch.2019.03.003

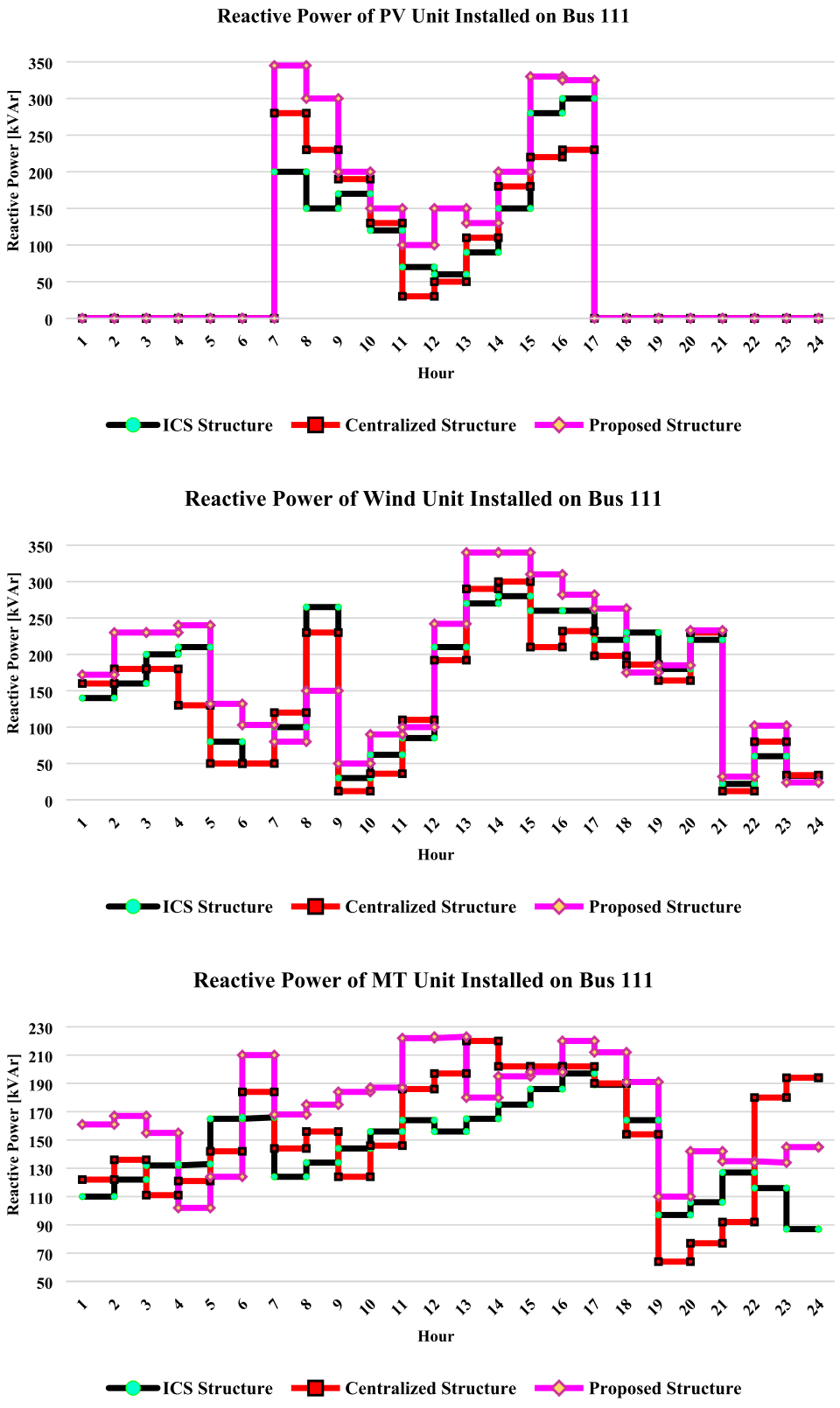

Fig. 12. Reactive power production of DERs of IEEE-33 bus ADG for a 24-hour period of time.

Please cite this article as: M. Hashemi and M. H. Zarif, A novel two-stage distributed structure for reactive power control, Engineering Science and Technology, an International Journal, https://doi.org/10.1016/j.jestch.2019.03.003

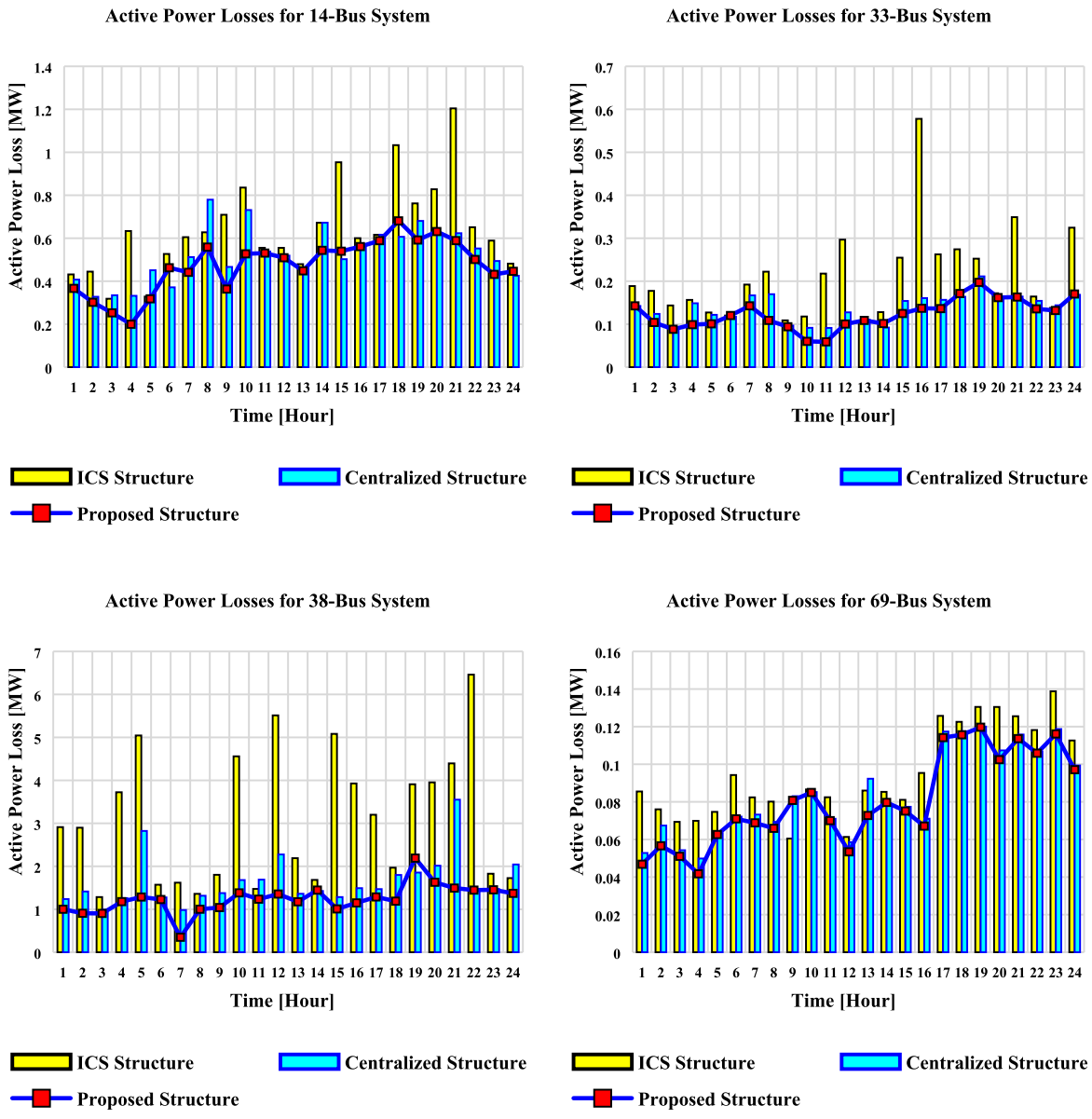

Fig. 13. Active power losses of the networks for a 24-hour period of time.

Please cite this article as: M. Hashemi and M. H. Zarif, A novel two-stage distributed structure for reactive power control, Engineering Science and Technology, an International Journal, https://doi.org/10.1016/j.jestch.2019.03.003

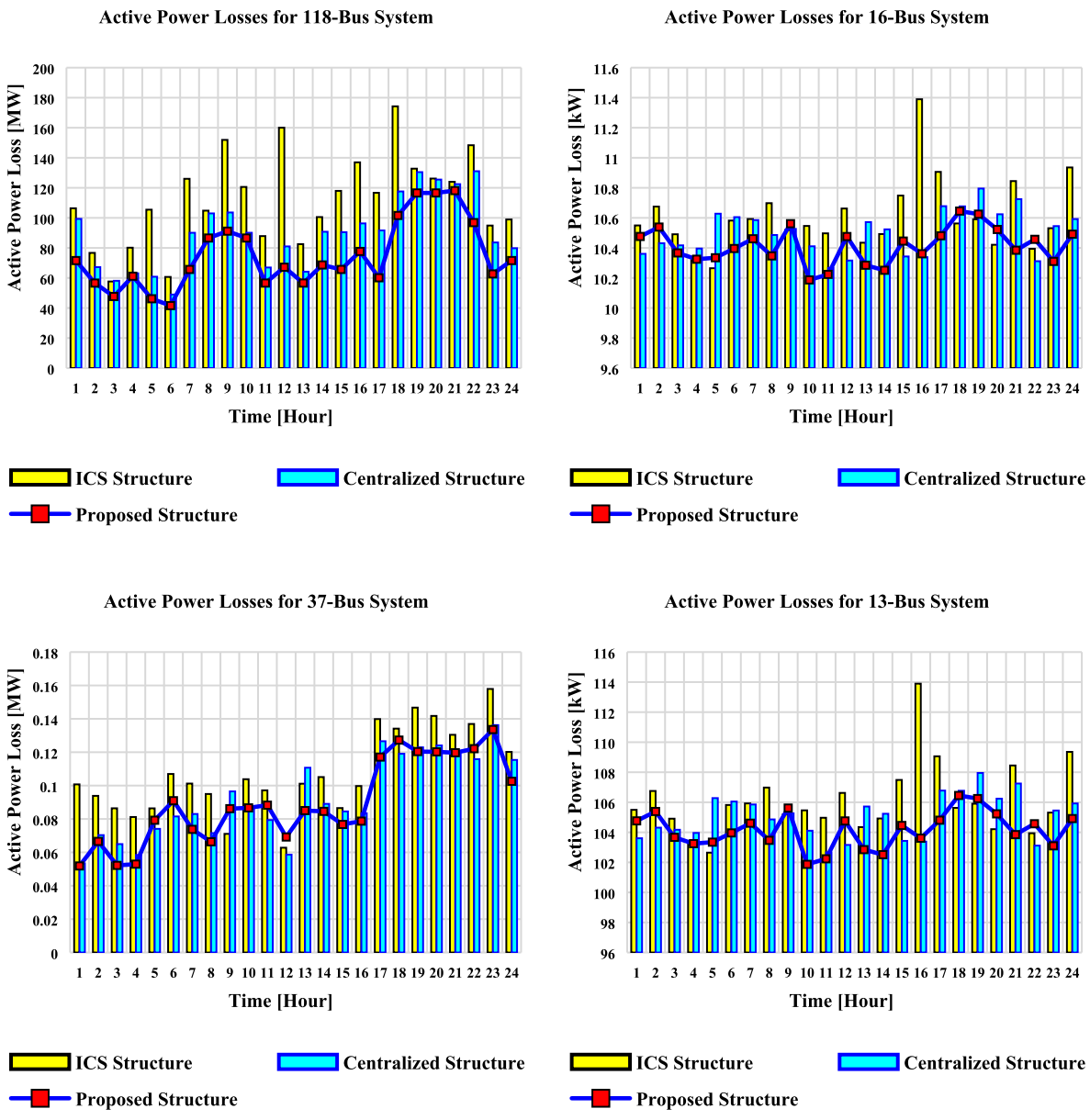

Fig. 13 (*continued*)

Please cite this article as: M. Hashemi and M. H. Zarif, A novel two-stage distributed structure for reactive power control, Engineering Science and Technology, an International Journal, https://doi.org/10.1016/j.jestch.2019.03.003

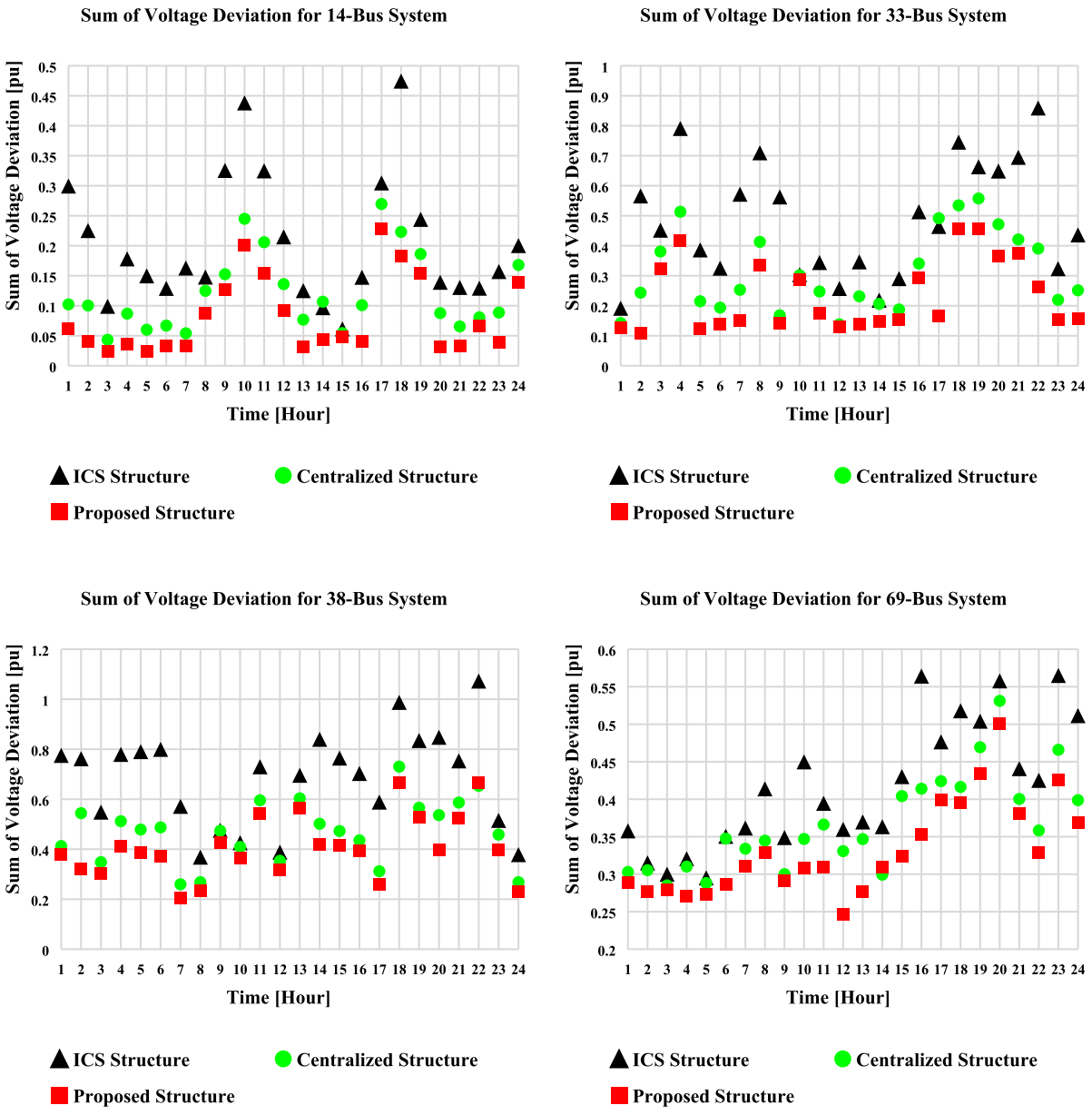

Fig. 14. Voltage deviation of the networks for a 24-hour period of time.

Please cite this article as: M. Hashemi and M. H. Zarif, A novel two-stage distributed structure for reactive power control, Engineering Science and Technology, an International Journal, https://doi.org/10.1016/j.jestch.2019.03.003

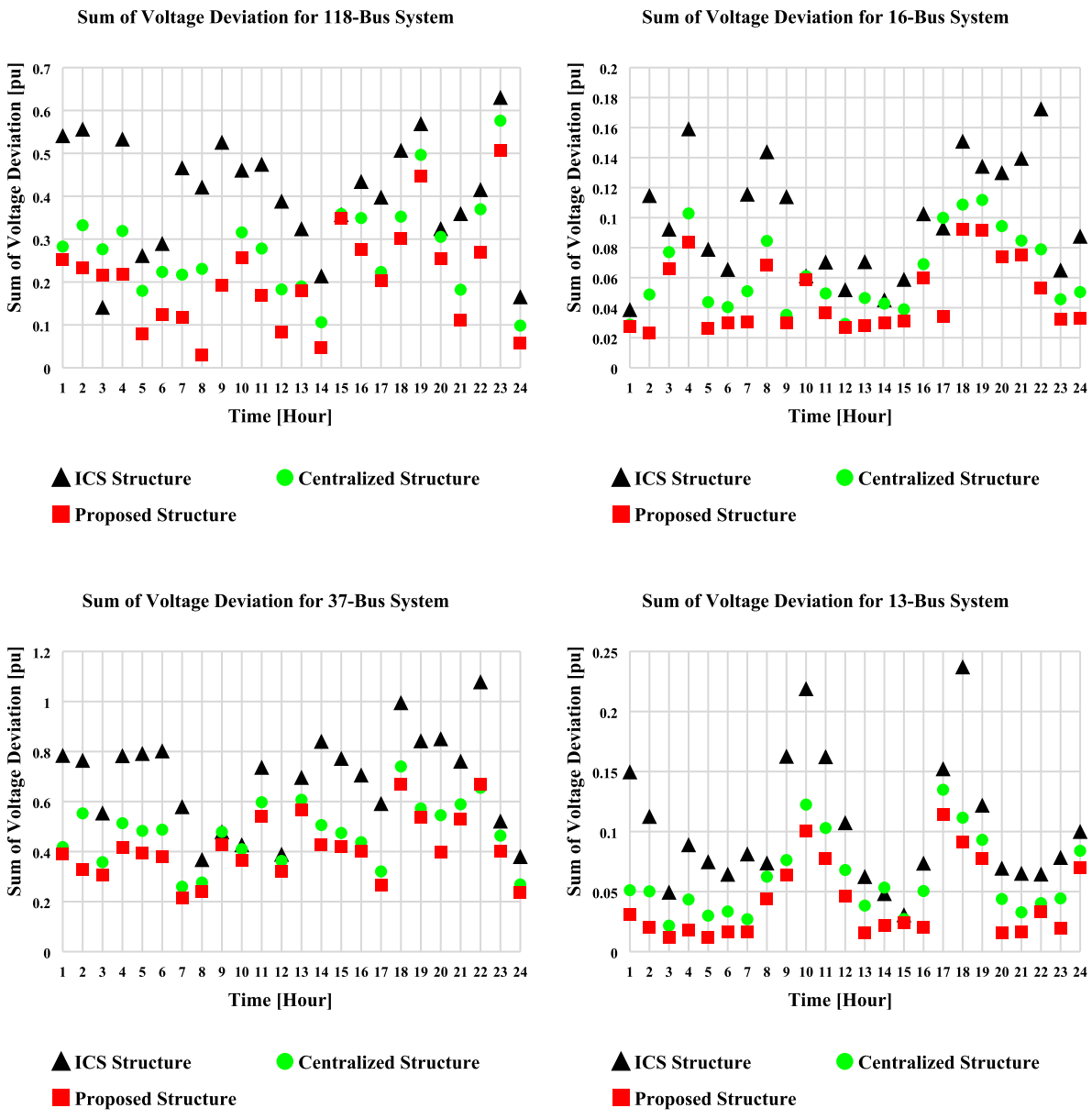

Fig. 14 (*continued*)

Please cite this article as: M. Hashemi and M. H. Zarif, A novel two-stage distributed structure for reactive power control, Engineering Science and Technology, an International Journal, https://doi.org/10.1016/j.jestch.2019.03.003

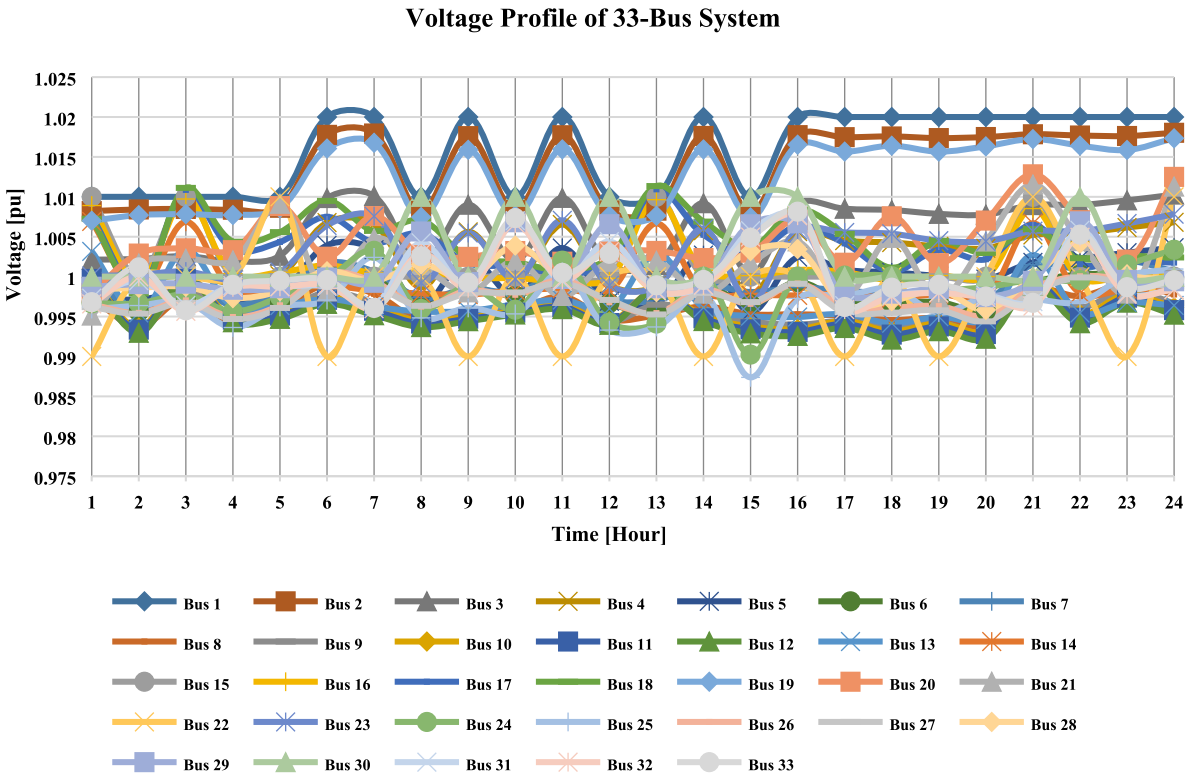

Fig. 15. The voltage profile of IEEE 33-bus ADG for a 24-hour period of time.

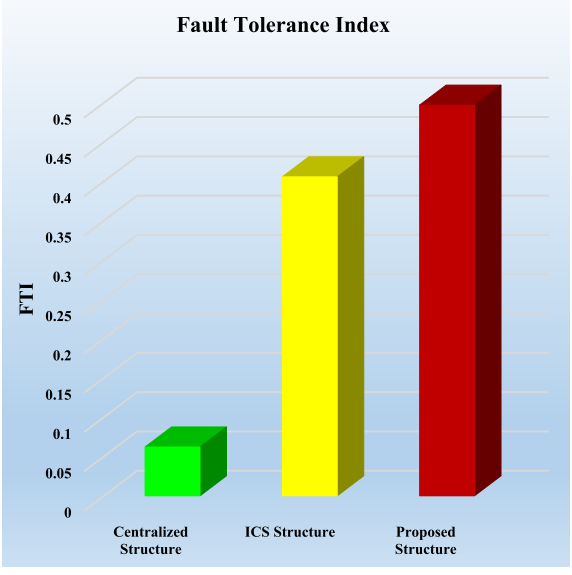

Fig. 16. FI index for different structures.

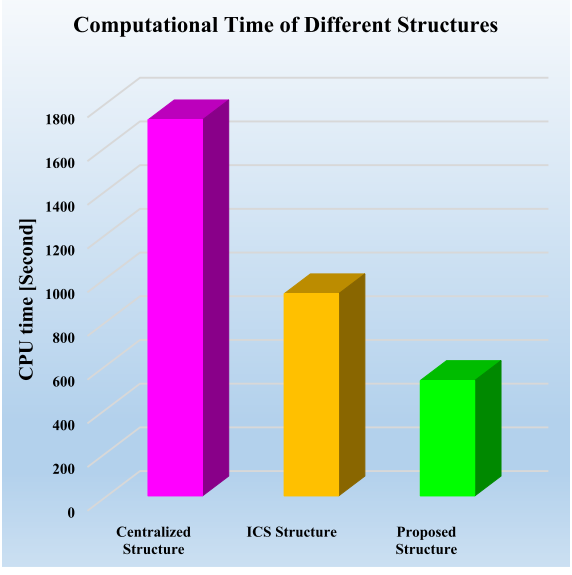

Fig. 17. Computational time for different structures.

Please cite this article as: M. Hashemi and M. H. Zarif, A novel two-stage distributed structure for reactive power control, Engineering Science and Technology, an International Journal, https://doi.org/10.1016/j.jestch.2019.03.003

References

[1] K. ben oualid Medani, S. Sayah, A. Bekrar, Whale optimization algorithm based optimal reactive power dispatch: a case study of the Algerian power system, Electr. Power Syst. Res. (2017).
[2] S.M. Mohseni-Bonab, A. Rabiee, Optimal reactive power dispatch: a review, and a new stochastic voltage stability constrained multi-objective model at the presence of uncertain wind power generation, IET Gener. Transm. Distrib. 11 (4) (2017) 815–829.
[3] Z. Yang, A. Bose, H. Zhong, N. Zhang, Q. Xia, C. Kang, Optimal reactive power dispatch with accurately modeled discrete control devices: a successive linear approximation approach, IEEE Trans. Power Syst. 32 (3) (2017) 2435–2444.
[4] M.G. Dozein, J. Ansari, H.R. Shahbazi, M. Kalantar, Optimal distribution voltage control through a sub-framework in the reactive power management on the Smart Grid, IEEE, 2013, pp. 153–159.
[5] M. Cavazzuti, Optimization Methods: From Theory to Design Scientific and Technological Aspects in Mechanics, Springer Science & Business Media, 2012.
[6] J. Ansari, M.G. Dozein, A. Kazemi, A novel voltage control strategy in collaboration with information technology domains through the holonic architecture, Turk. J. Electr. Eng. Comput. Sci. 24 (5) (2016) 4242–4253.
[7] D. Devaraj, Improved genetic algorithm for multi-objective reactive power dispatch problem, Int. Trans. Electr. Energy Syst. 17 (6) (2007) 569–581.
[8] J. Ansari, M. Jamei, A. Kazemi, Integration of the wind power plants through a novel, multi-objective control scheme under the normal and emergency conditions, Int. Trans. Electr. Energy Syst. 26 (8) (2016) 1752–1782.
[9] D.S. Stephen, P. Somasundaram, Solution for multi-objective reactive power optimization using fuzzy guided tabu search, Arab. J. Sci. Eng. 37 (8) (2012) 2231–2241.
[10] X.l. Tang, H. Zhang, Y.Q. Cui, L. Gu, Y.Y. Deng, A novel reactive power optimization solution using improved chaos PSO based on multi-agent architecture, Int. Trans. Electr. Energy Syst. 24 (5) (2014) 609–622.
[11] H. Karimi, J. Ansari, A. Gholami, A. Kazemi, A comprehensive well to wheel analysis of plug-in vehicles and renewable energy resources from cost and emission viewpoints, IEEE, 2014, pp. 1–6.
[12] S. Duman, Y. Sönmez, U. Güvenç, N. Yörükeren, Optimal reactive power dispatch using a gravitational search algorithm, IET Gener. Transm. Distrib. 6 (6) (2012) 563–576.
[13] Y. Li, Y. Wang, B. Li, A hybrid artificial bee colony assisted differential evolution algorithm for optimal reactive power flow, Int. J. Electr. Power Energy Syst. 52 (2013) 25–33.
[14] C. Dai, W. Chen, Y. Zhu, X. Zhang, Seeker optimization algorithm for optimal reactive power dispatch, IEEE Trans. Power Syst. 24 (3) (2009) 1218–1231.
[15] A. Rabiee, M. Vanouni, M. Parniani, Optimal reactive power dispatch for improving voltage stability margin using a local voltage stability index, Energy Convers. Manage. 59 (2012) 66–73.
[16] D.Q. Zhou, U.D. Annakkage, A.D. Rajapakse, Online monitoring of voltage stability margin using an artificial neural network, IEEE Trans. Power Syst. 25 (3) (2010) 1566–1574.
[17] H. Kazari, A.A.-T. Fard, A. Dobakhshari, A.M. Ranjbar, Voltage stability improvement through centralized reactive power management on the Smart Grid, in: Innovative Smart Grid Technologies (ISGT), 2012 IEEE PES, IEEE, 2012, pp. 1–7.
[18] A.A. Aquino-Lugo, R. Klump, T.J. Overbye, A control framework for the smart grid for voltage support using agent-based technologies, IEEE Trans. Smart Grid 2 (1) (2011) 173–180.
[19] J. Ansari, A. Gholami, A. Kazemi, Multi-agent systems for reactive power control in smart grids, Int. J. Electr. Power Energy Syst. 83 (2016) 411–425.
[20] M. Ghazavi Dozein, H. Monsef, J. Ansari, A. Kazemi, An effective decentralized scheme to monitor and control the reactive power flow: a holonic-based strategy, Int. Trans. Electr. Energy Syst. 26 (6) (2016) 1184–1209.
[21] A. Samimi, M. Nikzad, A. Kazemi, Coupled active and reactive market in smart distribution system considering renewable distributed energy resources and demand response programs, Int. Trans. Electr. Energy Syst. 27 (4) (2017).
[22] J. Ansari, A. Gholami, A. Kazemi, Holonic structure: a state-of-the-art control architecture based on multi-agent systems for optimal reactive power dispatch in smart grids, IET Gener. Transm. Distrib. 9 (14) (2015) 1922–1934.
[23] A.A. Aquino-Lugo, T. Overbye, Agent technologies for control applications in the power grid, in: System Sciences (HICSS), 2010 43rd Hawaii International Conference on, IEEE, 2010, pp. 1–10.
[24] K.M. Rogers, R. Klump, H. Khurana, A.A. Aquino-Lugo, T.J. Overbye, An authenticated control framework for distributed voltage support on the smart grid, IEEE Trans. Smart Grid 1 (1) (2010) 40–47.
[25] M. Granada, M.J. Rider, J. Mantovani, M. Shahidehpour, A decentralized approach for optimal reactive power dispatch using a Lagrangian decomposition method, Electr. Power Syst. Res. 89 (2012) 148–156.
[26] P. Pachanapan, O. Anaya-Lara, A. Dysko, K.L. Lo, Adaptive zone identification for voltage level control in distribution networks with DG, IEEE Trans. Smart Grid 3 (4) (2012) 1594–1602.
[27] W. Zhang, W. Liu, X. Wang, L. Liu, F. Ferrese, Distributed multiple agent system based online optimal reactive power control for smart grids, IEEE Trans. Smart Grid 5 (5) (2014) 2421–2431.
[28] M. Jamshidi, System of Systems Engineering: Innovations for the Twenty-First Century, John Wiley & Sons, 2011.
[29] D.P. Bertsekas, Nonlinear Programming, Athena scientific Belmont, 1999.
[30] Available: <https://www2.ee.washington.edu/research/pstca/pf118/pg_tca118bus.htm>.
[31] J.Z. Zhu, Optimal reconfiguration of electrical distribution network using the refined genetic algorithm, Electr. Power Syst. Res. 62 (1) (2002) 37–42.
[32] M.L. Pérez, Analysis and Operation of Smart Grids with Electric Vehicles, Universidad de Málaga, 2014.
[33] C. Yammani, S. Maheswarapu, S. Matam, Enhancement of voltage profile and loss minimization in distribution systems using optimal placement and sizing of power system modeled DGs, J. Electr. Syst. 7 (2011) 4.
[34] J.R. Castro, M. Saad, S. Lefebvre, D. Asber, L. Lenoir, Optimal voltage control in distribution network in the presence of DGs, Int. J. Electr. Power Energy Syst. 78 (2016) 239–247.
[35] X. Kong, J. Huang, C. Lin, P.D. Ungsunan, Performance, fault-tolerance and scalability analysis of virtual infrastructure management system, in: 2009 IEEE International Symposium on Parallel and Distributed Processing with Applications, IEEE, 2009, pp. 282–289.

Please cite this article as: M. Hashemi and M. H. Zarif, A novel two-stage distributed structure for reactive power control, Engineering Science and Technology, an International Journal, https://doi.org/10.1016/j.jestch.2019.03.003